Summer 2014

Key Residues of Human Cytoplasmic Protein Tyrosine Phosphatase-A and -B for Substrate Binding and Specificity

Byunghyun Park
Purdue University

Graduate School ETD Form 9
(Revised 01/14)

PURDUE UNIVERSITY
GRADUATE SCHOOL
Thesis/Dissertation Acceptance

This is to certify that the thesis/dissertation prepared

By Byunghyun Park

Entitled
KEY RESIDUES OF HUMAN CYTOPLASMIC PROTEIN TYROSINE PHOSPHATASE- A AND-B FOR SUBSTRATE BINDING AND SPECIFICITY

For the degree of Master of Science

Is approved by the final examining committee:

Cynthia V. Stauffacher

Sandra Rossie

Mark C. Hall

To the best of my knowledge and as understood by the student in the *Thesis/Dissertation Agreement. Publication Delay, and Certification/Disclaimer (Graduate School Form 32)*, this thesis/dissertation adheres to the provisions of Purdue University's "Policy on Integrity in Research" and the use of copyrighted material.

Cynthia V. Stauffacher

Approved by Major Professor(s): _____

Approved by: Jeffrey Lucas 07/09/2014

Head of the Department Graduate Program Date

Key Residues of Human Cytoplasmic Protein Tyrosine Phosphatase-A and -B for Substrate Binding and Specificity

A Dissertation
Submitted to the Faculty
of
Purdue University
by
Byunghyun Park

In Partial Fulfillment of the
Requirements for the Degree
of
Master of Science

August 2014
Purdue University
West Lafayette, Indiana

“MANY PEOPLE DIE AT TWENTY FIVE AND AREN’T BURIED UNTIL THEY ARE SEVENTY FIVE.”

- BENJAMIN FRANKLIN -

“YOUR TIME IS LIMITED, SO DON'T WASTE IT LIVING SOMEONE ELSE'S LIFE.”

- STEVE JOBS -

ACKNOWLEDGMENTS

I would love to thank my parents, Heesuk Kim and Kilsik Park for their love and encouragement. I would also like to thank my brother, Byungil Park for supporting me throughout grad school.

Next I would like to thank Dr. Cynthia Stauffacher for providing me the opportunity to challenge myself again. I would also like to thank my committee members: Dr. Mark Hall and Dr. Sandra Rossie for their helpful suggestions.

Finally I would like to thank my friends: my lab mates Kaibo Zhang, Chun-liang Chen, Qing Zhou, Tim Schmidt for all of the help, discussion and good times. I would also like to thank Sungun Huh, Hyun Sung, Yonggu Lee, Misun Jin, Saerom Park, Eunha Jung, Yongchae Park, Sujin Kim, Youngran Park, Heejin Yoo, Flowerstar Lee, and friends of Eastnation and all the other friends that made my graduate life a great memory.

TABLE OF CONTENTS

Page

LIST OF TABLES

LIST OF FIGURES

Figure Page

Figure Page

LIST OF ABBREVIATIONS

ABBREVIATION	DESCRIPTION
ACP1	Acid Phosphatase 1
Arg (R)	Arginine
Asn (N)	Asparagine
ATP	Adenosine Triphosphate
CD45	Protein tyrosine phosphatase, receptor type, C
DTT	Dithiothreitol
DMSO	Dimethyl Sulfoxide
EDTA	Ethylenediaminetetraacetic acid
PMSF	Phenylmethanesulfonylfluoride or Phenylmethylsulfonyl Fluoride
E. coli	Escherichia coli
Glu (E)	Glutamic Acid
HCPTP	Human Cytoplasmic Protein Tyrosine Phosphatase
IPTG	Isopropyl β-d-1-thiogalactopyranoside
IEC	Ion Exchange Chromatography
LB	Lewy body
PCR	Polymerase Chain Reaction
*p*NPP	*p*-Nitrophenyl Phosphate
PTPs	Protein Tyrosine Phosphatases
PTEN	Phosphatase and Tensin Homolog
RTK	Receptor Tyrosine Kinase
SAM	Sterile Alpha Motif
SDS-PAGE	Sodium Dodecyl Sulfate Polyacrylamide Gel Electrophoresis
SEC	Size Exclusion Chromatography
Tyr (Y)	Tyrosine
Trp (W)	Tryptophan
WT	Wildtype

ABSTRACT

Park, Byunghyun. M.S., Purdue University, August 2014. Key Residues of Human Cytoplasmic Protein Tyrosine Phosphatase- A and -B for Substrate Binding and Specificity. Major Professor: Cynthia Stauffacher.

Reversible tyrosine phosphorylation plays an important role in signaling pathways that are essential for regulating cellular growth, differentiation and metabolism. Moreover, several human diseases such as diabetes, obesity and cancers are associated with the deregulation of protein tyrosine phosphatases (PTPs). Several studies provide evidence that PTPs not only contribute to cellular differentiation, but over-expression of these molecules also leads to transformation of non-transfomed cells as well. Based on these results, designing specific PTP inhibitors may ultimately function as potential therapeutic agents to treat various diseases including cancer, diabetes, and autoimmune diseases. EphA2 is a receptor tyrosine kinase which is hypo-phosphorylated and overexpressed in many metastatic cancers. The level of phosphorylation of EphA2 is controlled by the human cytoplasmic protein tyrosine phosphatase (HCPTP), which is also overexpressed in cancers. Two low molecular weight PTP isoenzymes, HCPTP-A and HCPTP-B, are generally expressed in humans. Interestingly, HCPTP-A and -B preferentially dephosphorylate different phosphotyrosine sites related to control of EphA2 activity and downstream signaling pathways. In addition, HCPTP-A and HCPTP-B have highly different activities towards substrates including *p*NPP and inhibitors. However, research to determine each characteristic of HCPTP-A and HCPTP-B, has not been done. Our research aims to shed light upon the key residues of HCPTP-A and HCPTP-B for substrate binding and activity through the use of site-directed mutagenesis. Because both EphA2 and HCPTP are related to cancer, revealing key residues that control the affinity of specific substrates to HCPTP-A and -B may yield an advance in understanding the biological roles of HCPTP as well as contributing to the development of rational HCPTP inhibitors for therapeutic treatment.

CHAPTER 1. INTRODUCTION

1.1. Human Cytoplasmic Protein Tyrosine Phosophatase

Human cytoplasmic protein tyrosine phosphatase (HCPTP) was initially identified as an acid phosphatase from red blood cells (1). The human ACP1 gene, located on the short arm of choromosome 2, includes 7 exons and 6 introns (2). Four isoforms of HCPTP arise from an alternative splicing of a primary transcript. Three mRNAs encode for HCPTP-A, -B, and -C in Figure 1.1 (3). HCPTP-A and HCPTP-B are active isoforms, resulting from mutually exclusive retention of exon 3f (in HCPTP-A) or exon 3s (in HCPTP-B) (4). However, HCPTP-C is an inactive protein, which has neither exon 3 nor exon 4 (5). The HCPTP-A and HCPTP-B show different electrophoretic mobility. While HCPTP-A electrophoretically migrates more slowly, HCPTP-B shows fast electrophoretic mobility (6). Moreover, they have different activity towards inhibitors and phosphotyrosine peptides (7). HCPTP-A has a higher activity towards phosphotyrosine, *p*-Nitrophenyl Phosphate (*p*NPP) and inhibitors, while HCPTP-B shows a lower response to *p*NPP and phosphotyrosine as well as inhibitors.

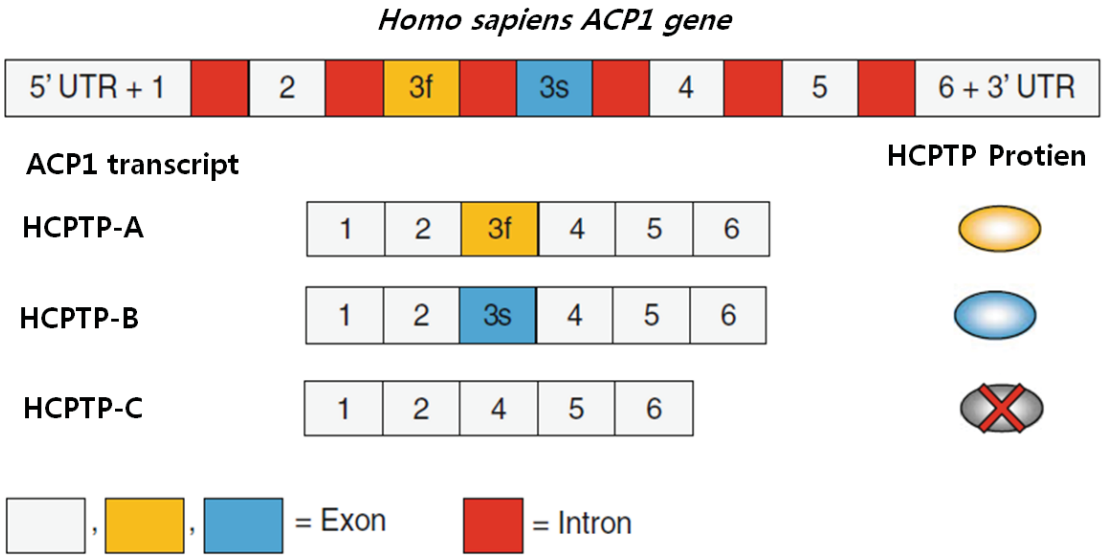

Figure 1.1. Isoforms of HCPTP (3). Alternative splicing of the ACP1 pre-mRNA leads to HCPTP-A, HCPTP-B, and HCPTP-C. HCPTP-A and -B result from mutually exclusive retention of the third exon (3f in HCPTP-A), or the fourth exon (3s in HCPTP-B). HCPTP-C is a catalytically inactive isoform (removal of both exon 3f and 3s).Image modified from Stephanie M. Stanford *et al*. 2013 (3).

1.1.1. HCPTP Structure and Function

The HCPTP-A and -B are soluble proteins with molecular mass of approximately 18,000 Da. They consist of single polypeptide chains of 157 amino acids and have identical sequence including the PTPase consensus sequence CX_5R which forms the active site P loop. The only different sequence between HCPTP-A and -B is an mRNA splice variant sequence containing amino acids 40 - 73 which forms the variable loop as shown in Figure 1.2 (8). The structure of HCPTP isoforms comprise a four-stranded central parallel β sheet and contain flanking α-helices on both sides which show two right-handed βαβ motifs as seen in Figure 1.3 (8).

Despite HCPTP-A and -B showing the structurally similar active site including the CX_5R, universal PTPase consensus sequence, they have different activity towards inhibitors and phosphotyrosine peptides (7). Moreover, HCPTP-A and -B preferentially dephosphorylate different phosphotyrosine sites related to control of EphA2 activity and downstream signaling pathways (9). By using a mass spectrometry-based assay, Balasubramaniam *et al*. showed the HCPTP-A and HCPTP-B have different dephosphorylation rates at the phosphotyrosine sites associated with control of EphA2 activity (Figure 1.4). It was illustrated that tyrosine Y772 of the kinase domain is dephosphorylated about 6 times faster by HCPTP-A, while tyrosine Y960 of the SAM domain is dephosphorylated only by HCPTP-B. Balasubramaniam *et al*. demonstrated in Figure 1.5 the kinase domain tyrosine, Y772 is the preferred target for dephosphoylation by HCPTP-A and the SAM domain tyrosine, Y960 is a site for dephosphorylation only by HCPTP-B (9).

Based on the preliminary study, three potential variable loop residues (49, 50, and 53) may influence the enzyme activity and substrate binding for HCPTP-A and -B in Figure 1.6 (7). Residue 49, which is Tyrosine (Tyr) in HCPTP-A and Tryptophan (Trp) in HCPTP-B, located above the active site forming the hydrophobic sandwich with residues Tyr-131 and -132, affects interaction of the ring portion of phosphotyrosine substrates. Residues 50 and 53 contribute to the difference of the variable loops charge distribution. Residue 50, Glutamic Acid (Glu) in HCPTP-A, contains a negatively charged side chain, whereas, residue 53, which is Arginine (Arg) in HCPTP-B, possesses a positively charged side chain. These two residues, 50 and 53, are important for the interaction of enzymes and substrates recognized by their charge distribution.

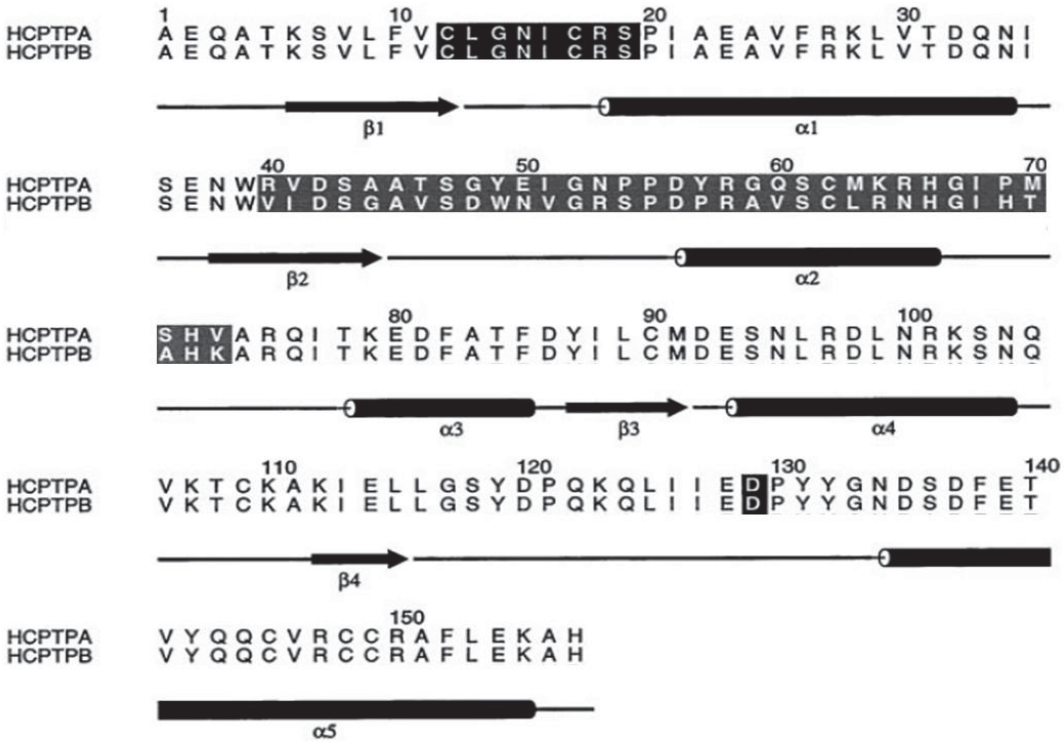

Figure 1.2. Sequence alignment of HCPTP-A and HCPTP-B (8).
Secondary structure elements were shown under the sequences. Critical catalytic residues are highlighted in black. The PTPase consensus sequence CX_5R (appears as sequence CLGNICRS) forms the active site P loop (black highlighting). The variable sequence between residues 40 and 73 forms the variable loop (gray highlighting). Image reproduced with permission from the copyright holder.

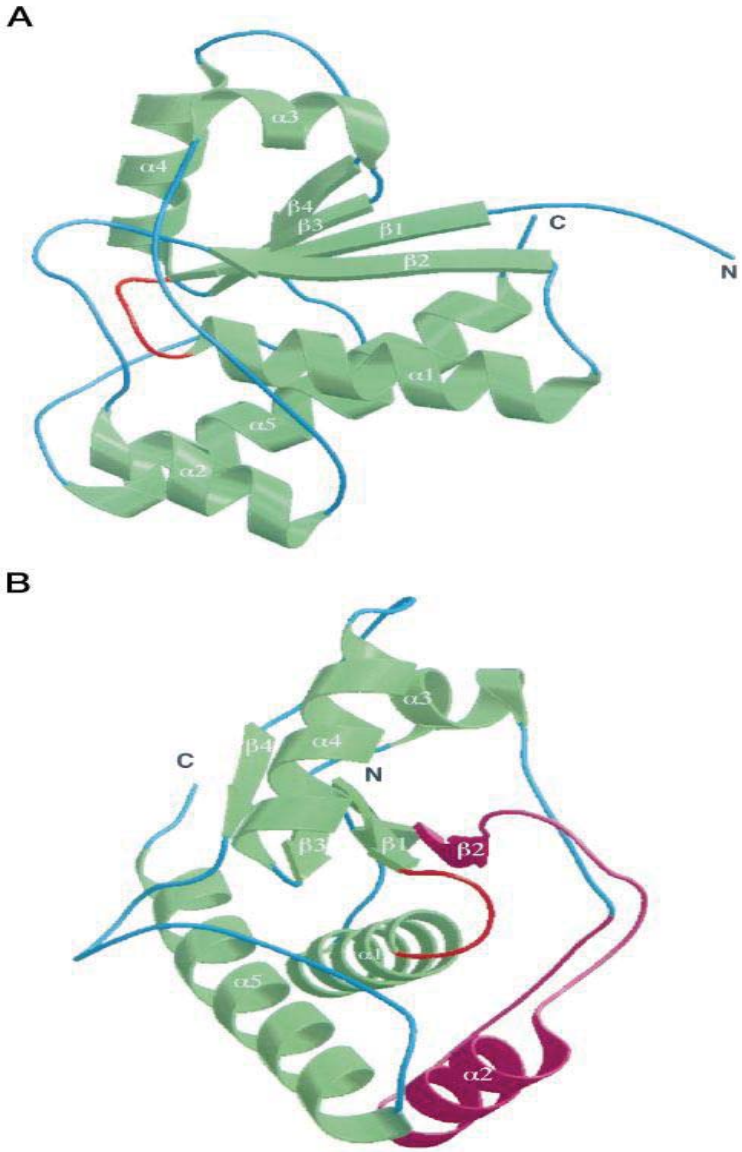

Figure 1.3. Ribbon diagrams of the fold of HCPTP-A (8).
A) The active site P loop (in red) connecting the first β strand (β1) to the first turn of the helix, α1. B) The variable loop (in purple) includes β2, the loop connecting β2 and α2, the helix α2, and part of the loop after α2. Image reproduced with permission from the copyright holder.

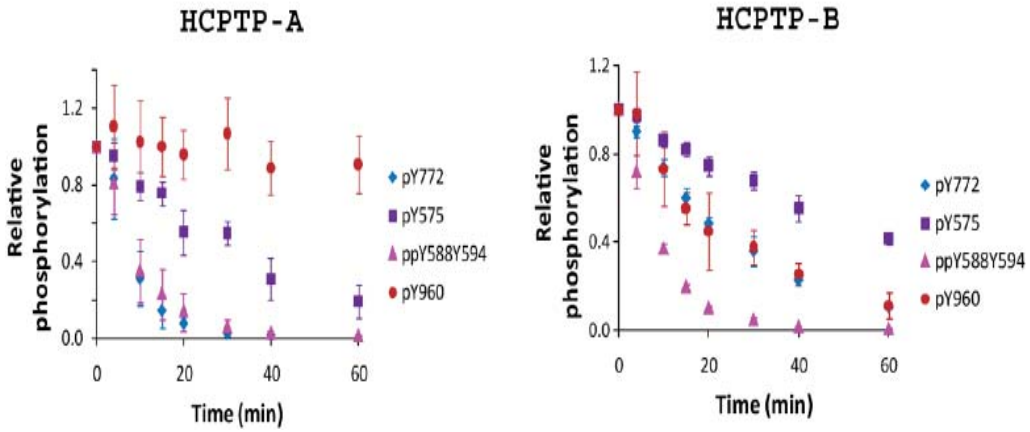

Figure 1.4. Dephosphorylation rates of the two HCPTP variants toward EphA2 phospho-peptides (9). SRM-MS analysis was used to determine the dephosphorylation rates of HCPTP-A (Left) and HCPTP-B (Right) against EphA2 phosphotyrosine peptides. Phosphorylation of sample at time 0 was adjusted to 100% and the percentage phophorylation was plotted relative to 0 minutes. Image modified from Balasubramaniam *et al*. 2011. Image reproduced with permission from the copyright holder.

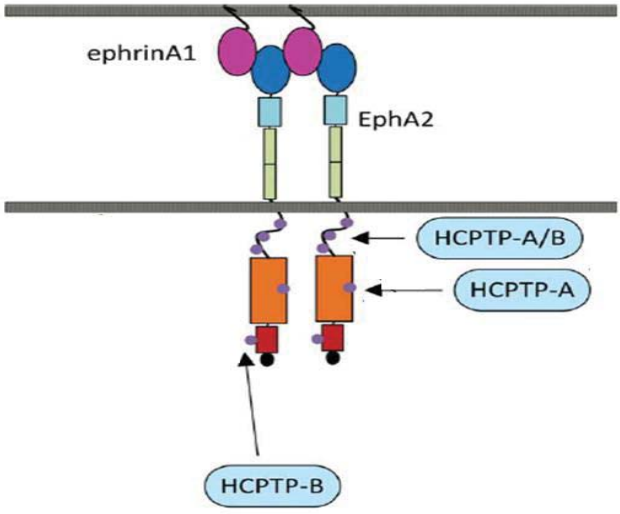

Figure 1.5. Specificity of HCPTP-A and -B against EphA2 tyrosines (9). The unstructured loop is the juxtamembrane region with three phosphorylated tyrosines marked by purple circle. The kinase domain of EphA2 is drawn in orange followed by the SAM domain shown in red with tyrosine marked by purple circle. The kinase domain tyrosine is a preferred target for dephosphorylation by HCPTP-A. The tyrosine in the SAM domain is a target for dephosphorylation exclusively by HCPTP-B. Image modified from Balasubramaniam *et al*. 2011. Image reproduced with permission from the copyright holder.

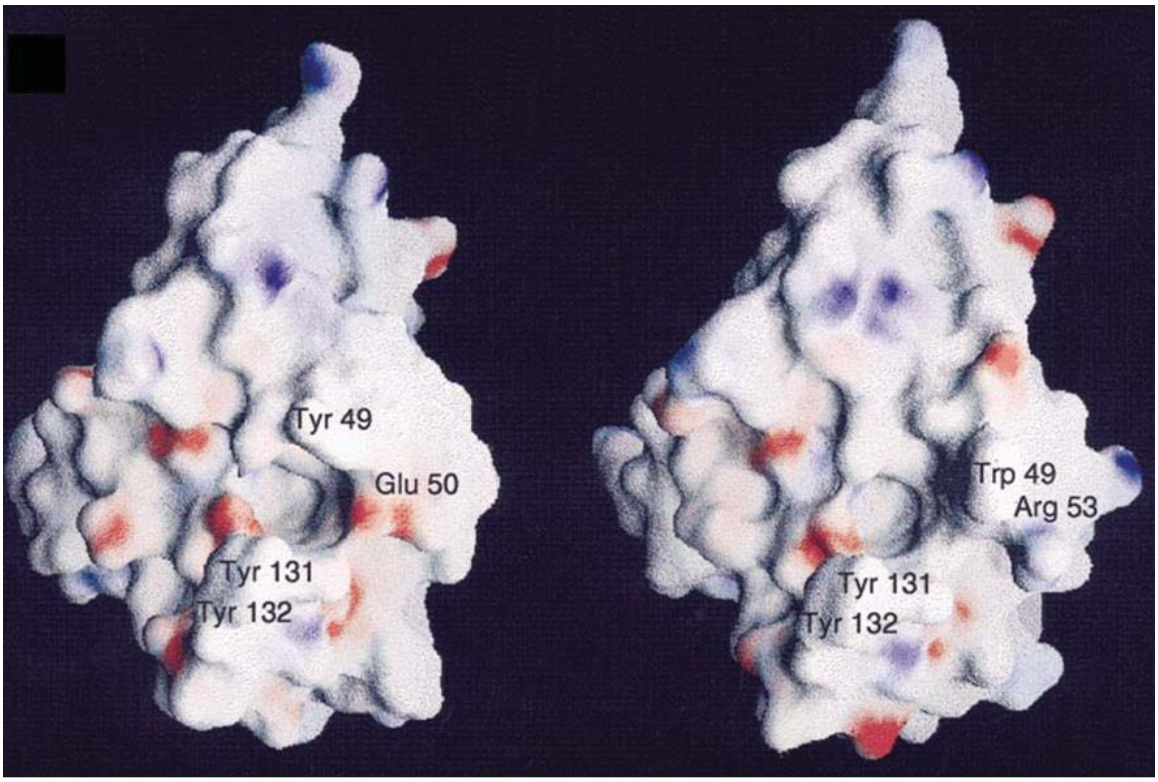

Figure 1.6. Electrostatic surface representation of HCPTP-A (left) and HCPTP-B (right) (7). The entrance to the active site appears as a circular depression at the center of the molecule. The crevice leading into the active-site pocket from the lower right is supposed to be the peptide biding site. The most dramatic charge alteration on the surface is near the active site, due to changes in residues 50 and 53, which border the crevice. Glu-50 in HCPTP-A contains a negatively charged side chain, whereas, Arg-53 in HCPTP-B possesses a positively charged side chain. Charge distributions are indicated by red (negative) and blue (positive). Image modified from Adam P. R. Zabell *et al*. 2005. Image reproduced with permission from the copyright holder.

1.1.2. HCPTP in Cancer and Diseases

EphA2 is a receptor tyrosine kinase which is hypo-phosphorylated and overexpressed in many metastatic cancers. The level of phosphorylation of EphA2 is regulated by the human cytoplasmic protein tyrosine phosphatase (HCPTP), which is also overexpressed in cancers as seen in Figure 1.7 (10). This indicates that HCPTP has oncogenic potential and seems to play an important role in metastatic transformation.

Moreover, several PTPs have been associated with many diseases including obesity, autoimmune and infectious diseases. A mutated SHP-1 (Src homology 2-containing tyrosine phosphatase) gene leads to severe immune dysfunction in mice (11). T lymphocytes with a mutated CD45 (Protein tyrosine phosphatase, receptor type, C) gene are irresponsive to stimulation by antigen and it might be related to autoimmune diseases (12). PTP1B and PTPα function as negative regulators of insulin signaling and they are involved in Type II diabetes and obesity (13).

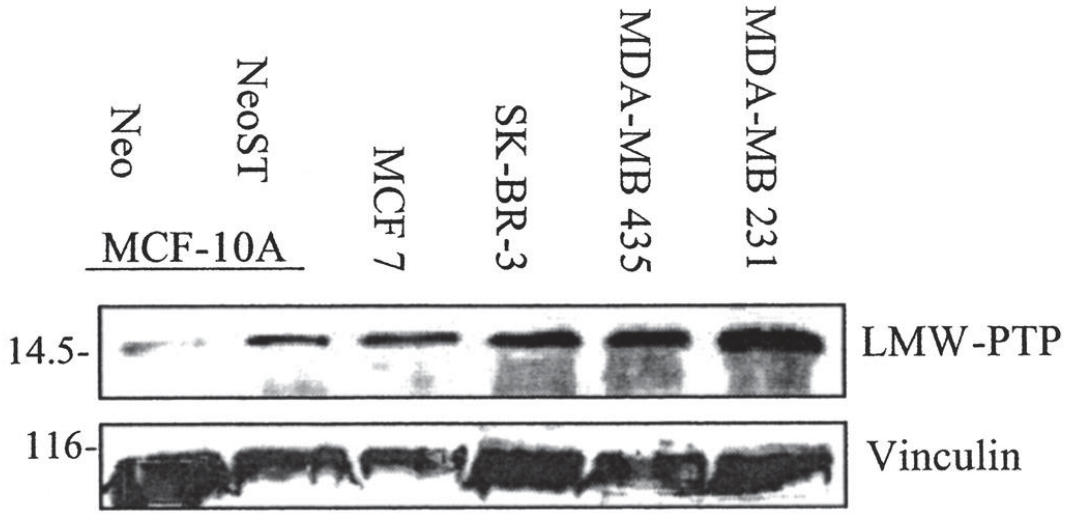

Figure 1.7. HCPTP levels are elevated in transformed cell lines. (10) Detergent lysates from various cell lines were probed for HCPTP. Oncogene-transformed cells (MCF7, SK-BR-3, MDA-MB-435, and MDA-MB-231) overexpress HCPTP compared to non-transformed cells (MCF-10AneoST denoted as NeoST). Image reproduced with permission from the copyright holder.

Table 1. Overview of PTPs that are potential therapeutic targets, grouped by disease area

Disease area	PTP
Autoimmune diseases	CD45
Infectious diseases	SHP1, SHP2
Obesity and diabetes	PTP1B
Cancer	PTP-α
Neurodegeneration	PTP1B

Table 1. Overview of PTPs that are potential therapeutic targets (12). Image modified from Rob Hooft van Huijsduijnen et al. 2002.
Abbreviations: SHP, Src homology 2-containing tyrosine phosphatase

1.2. Purpose

Interest in PTPs began to rise because PTPs play critical roles in the regulation of various cellular signaling pathways and they emerged as potential drug targets for several disease areas in Table 1 (14). Designing specific PTP inhibitors will ultimately function as potential therapeutic agents to treat various diseases including cancer, obesity, and autoimmune diseases.

However, developing rational PTP inhibitors for therapeutic treatment is considered to be a challenging task. First, because a large number of PTPs have the consensus sequence CX_5R, which forms the active site, it seems improbable that specifically designed inhibitors would selectively target only one PTP. Second, PTP inhibition may lead to unwanted side-effects because a key signaling pathway may be regulated by various PTPs or a single PTP may regulate diverse cellular signaling pathways.

The following experiments were performed to understand the key residues of HCPTP-A and HCPTP-B for substrate binding and activity and help answer major concerns in designing of rational PTP inhibitors.

Two low molecular weight PTP isoenzymes, HCPTP-A and HCPTP-B, are generally expressed in human. These two enzymes, HCPTP-A and B have highly identical sequences except for the variable loop (residues 40 - 73) region, which determines its binding substrates leading either to an inhibitor or activator response. Based on the preliminary study, using biochemical substrates and inhibitors as well as analyzing the structure, our lab identified with three potential variable loop residues (49, 50, and 53) that may influence the determination of catalytic efficiency and substrate binding for HCPTP-A and -B. Thus, a major goal of this project is investigating the effect of these residues on HCPTP-A and -B activity through site-directed mutations of residues 49, 50, and 53. This will provide a more detailed understanding of specific residues that control the affinity of substrates for the PTPs. Moreover, understanding which residue plays a critical role in substrate binding and activity for HCPTP-A and -B may yield an advance in understanding the biological roles of PTPs as well as contributing to the development of effective drug candidates against HCPTP.

CHAPTER 2. CLONING, EXPRESSION, AND PURIFICATION OF THE HCPTP-A AND -B WILD TYPE, SINGLE, DOUBLE, AND TRIPLE MUTANTS

2.1. Introduction

Two low molecular weight PTP isoenzymes, HCPTP-A and HCPTP-B, are soluble proteins with molecular mass of approximately 18 kDa. HCPTP-A and -B consist of single polypeptide chains of 157 amino acids and have universal PTPase consensus sequence CX_5R that forms the active site P loop. The only distinct sequence between HCPTP-A and HCPTP-B consists of residues 40-73 which forms the variable loop (8). Despite HCPTP-A and -B showing a structurally similar active site including the universal PTPase consensus sequence, they show different activity against inhibitors and phosphotyrosine peptides (7). Moreover, it was recently shown that HCPTP-A and -B preferentially dephosphorylate different phosphotyrosine sites related to control of EphA2 activity and downstream signaling pathways. HCPTP-A preferentially dephosphorylates tyrosine Y772 of the kinase domain in the activation loop, while HCPTP-B preferentially dephosphorylates the SAM domain tyrosine, Y960. (9) However, which residues of HCPTP-A and -B are responsible for different activity toward phosphotyrosine sites of EphA2 still remains unknown.

Based on the preliminary study, our lab identified three potential variable loop residues (49, 50, and 53) that may influence the determination of enzymatic activity and substrate binding for HCPTP-A and -B. Residue 49, which is Tyr(Y) in HCPTP-A and Trp(W) in HCPTP-B, located above the active site forming the hydrophobic sandwich with residues Tyr-131 and -132, affects interaction of the ring portion of phosphotyrosine substrates. Residues 50 and 53 contribute to the difference of the variable loops charge distribution. Glu(E)-50 in HCPTP-A, contains a negatively charged side chain, whereas, Arg(R)-53 in HCPTP-B, possesses a positively charged side chain. These two residues,

50 and 53, are important for the interaction of enzymes and substrates recognized by their charge distribution. Thus, investigating the effect of these residues on HCPTP-A and -B activity through site-directed mutations of residues 49, 50, and 53 will provide a more detailed understanding of specific residues that control the affinity of substrates to both HCPTP-A and -B and contribute to the development of effective drug candidates against HCPTP.

2.2. Methods

2.2.1. Cloning HCPTP-A and -B, Single, Double, and Triple Mutants

Our lab already has vector pET11d containing the plasmid of HCPTP-A, A-Y49W, E50N, N53R, A-Y49W/E50N and HCPTP-B, B-W49Y, N50E, R53N, B-W49Y/N50E, respectively. These plasmids were used as templates for the polymerase chain reaction (PCR) to yield other types of double and triple mutants via site-directed mutagenesis.

Site-directed mutagenesis was carried out to make HCPTP-A E50N/N53R using pET11d vector containing HCPTP-A E50N template DNA with forward and reverse primers: 5' - CAA CTT CCG GGT ATA ACA TAG GGC GCC CCC CTG - 3' and 5' - CAG GGG GGC GCC CTA TGT TAT ACC CGG AAG TTG - 3', respectively. HCPTP-A Y49W/N53R was yielded from pET11d::HCPTP-A Y49W template plasmid using the following forward primers 5' - CAA CTT CCG GGT GGG AGA TAG GGC GCC - 3' and reverse primers 5' - GGC GCC CTA TCT CCC ACC CGG AAG TTG - 3'.To create HCPTP-A Y49W/E50N/N53R, site-directed mutagenesis was performed using HCPTP-A Y49W/E50N as template plasmid with forward and reverse primers: 5' - CTT CCG GGT GGA ACA TAG GGC GAC CCC CTG ACT ACC - 3' and 5 '- GGT AGT CAG GGG GTC GCC CTA TGT TCC ACC CGG AAG - 3'.

HCPTP-B N50E/R53N was PCR amplified from pET11d::HCPTP-B N50E template with forward primers 5' - CTG TTT CTG ACT GGG AGG TGG GCA ACT CCC CAG - 3' and reverse 5' - CTG GGG AGT TGC CCA CCT CCC AGT CAG AAA CAG - 3'. In order to yield HCPTP-B W49Y/R53N, HCPTP-B W49Y was used as template DNA for site-directed mutagenesis with forward and reverse primers: 5' - GCG GTG CTG TTT CTG ACT ATA ACG TGG GCA ACT CCC CAG - 3' and 5' - CTG GGG AGT TGC CCA CGT TAT AGT CAG AAA CAG CAC CGC - 3'. HCPTP-B W49Y/N50E/R53N was created from pET11d::HCPTP-B W49Y/N50E using site-directed mutagenesis with forward primers 5' - GTT TCT GAC TAT GAG GTG GGC AAC TCC CCA GAC CCA AGA GCT GTG - 3' and reverse primers 5' - CAC AGC TCT TGG GTC TGG GGA GTT GCC CAC CTC ATA GTC AGA AAC - 3', respectively (Table 2 - Table 3).

The PCR sample contained 1 ul of 10 uM forward and reverse primer, 1 ul template DNA, 0.4 ul of 10 mM dNTPs, 0.6 ul DMSO, 4 ul 5x Phusion GC buffer, 0.2 ul

Phusion DNA polymerase, and 11.8 ul nuclease free water. 20 cycles of PCR were performed for 50 seconds at 98°C for denaturation, 50 seconds at 60°C for annealing, and 6 minutes 30 seconds at 72°C for elongation (Figure 2.1.). Following the reaction, the PCR product was digested with DpnI to cleave methylated sites of the template plasmid but not the PCR product.

The 4 ul of PCR product were transformed into 20 ul *E.coli* XL-1 Blue competent cells each for 45 minutes on ice. The mixture was heat shocked at 42°C for 40 - 45 seconds and allowed to recover on ice for 5 minutes, at which point 500 ul of Luria broth (LB) media was added to the sample. That was then placed in the incubator at 37°C for 45 minutes, 220 rpm. 200 ul of the sample was spread on a Luria agar plate containing 50 ug/ml ampicilin and allowed to incubate overnight at 37°C. LB media is made by dissolving 10 g NaCl, 10 g tryptone, and 5 g yeast extract in 1000 mL deionized water, which is then autoclaved.

Colonies was selected from each transformation and used to inoculate 10 mL overnight cultures, that were subsequently pelleted. Plasmid DNA was isolated from the pellets using a Qiagen miniprep kit. Each sample was then sent for sequencing to confirm the presence of the desired mutation.

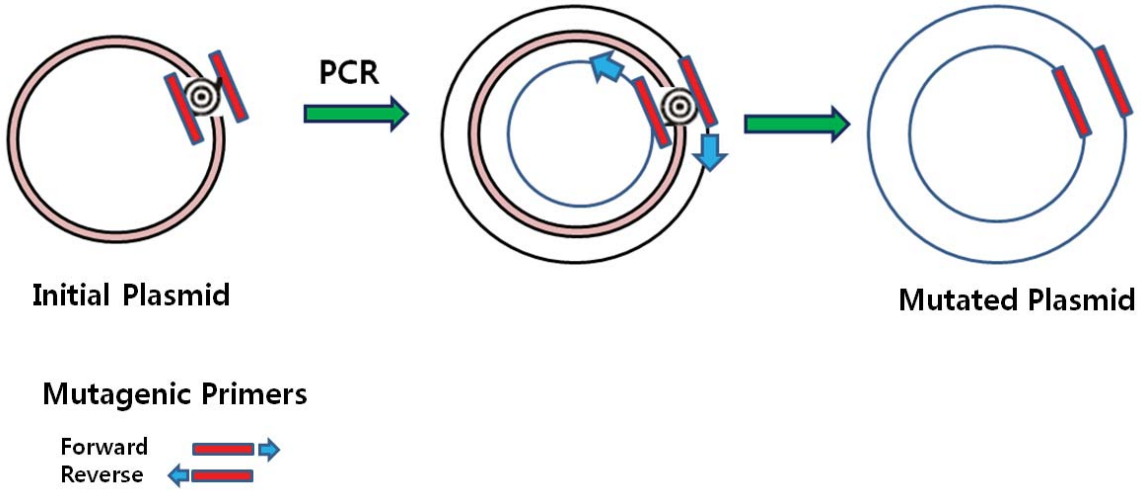

Figure 2.1. Site-directed mutagenesis for HCPTP-A E50N/N53R, Y49W/N53R, Y49W/E50N/N53R, and HCPTP-B N50E/R53N, W49Y/R53N, W49Y/N50E/R53N. HCPTP-A E50N, Y49W, Y49W/E50N and HCPTP-B W49Y, N50E, W49Y/N50E plasmids were used as templates for the polymerase chain reaction (PCR) to yield other types of double and triple mutants via site-directed mutagenesis. 20 cycles of PCR were performed for 50 seconds at 98°C, 50 seconds at 60°C, and 6 minutes 30 seconds at 72°C. Following the reaction, the PCR product was digested with DpnI.

Table 2. List of mutated, template plasmid, and primers.

Mutated plasmid	Template plasmid	Primers
A-E50N/N53R	**A-E50N**	**Forward** : 5'- CAA CTT CCG GGT ATA ACA TAG GGC GCC CCC CTG -3' **Reverse**: 5'- CAG GGG GGC GCC CTA TGT TAT ACC CGG AAG TTG -3'
A-Y49W/N53R	**A-Y49W**	**Forward** :5'- CAA CTT CCG GGT GGG AGA TAG GGC GCC- 3' **Reverse**: 5'- GGC GCC CTA TCT CCC ACC CGG AAG TTG- 3'
A-Y49W/E50N/N53R	**A-Y49W/E50N**	**Forward**: 5'- CTT CCG GGT GGA ACA TAG GGC GAC CCC CTG ACT ACC- 3' **Reverse**:5'- GGT AGT CAG GGG GTC GCC CTA TGT TCC ACC CGG AAG- 3'
B-N50E/R53N	**B-N50E**	**Forward**: 5'- CTG TTT CTG ACT GGG AGG TGG GCA ACT CCC CAG- 3' **Reverse**: 5'- CTG GGG AGT TGC CCA CCT CCC AGT CAG AAA CAG- 3'
B-W49Y/R53N	**B-W49Y**	**Forward**: 5'- GCG GTG CTG TTT CTG ACT ATA ACG TGG GCA ACT CCC CAG- 3' **Reverse**: 5'- CTG GGG AGT TGC CCA CGT TAT AGT CAG AAA CAG CAC CGC- 3'
B-W49Y/N50E/R53N	**B-W49Y/N50E**	**Forward**: 5'- GTT TCT GAC TAT GAG GTG GGC AAC TCC CCA GAC CCA AGA GCT GTG- 3' **Reverse**: 5'- CAC AGC TCT TGG GTC TGG GGA GTT GCC CAC CTC ATA GTC AGA AAC- 3'

Table 3. Sequencing alignment of HCPTP -A and -B , single, double, and triple mutants

Protein	Sequence (49 50 53)	Protein	Sequence (49 50 53)
A-WT	RVDSAATSGY EIGNPPDYRG	**B-WT**	VIDSGAVSDW NVGRSPDPRA
A-Y49W	RVDSAATSGW EIGNPPDYRG	**B-W49Y**	VIDSGAVSDY NVGRSPDPRA
A-E50N	RVDSAATSGY NIGNPPDYRG	**B-N50E**	VIDSGAVSDW EVGRSPDPRA
A-N53R	RVDSAATSGY EIGRPPDYRG	**B-R53N**	VIDSGAVSDW NVGNSPDPRA
A-Y49W/E50N	RVDSAATSGW NIGNPPDYRG	**B-W49Y/N50E**	VIDSGAVSDY EVGRSPDPRA
A-Y49W/N53R	RVDSAATSGW EIGRPPDYRG	**B-W49Y/R53N**	VIDSGAVSDY NVGNSPDPRA
A-E50N/N53R	RVDSAATSGY NIGRPPDYRG	**B-N50E/R53N**	VIDSGAVSDW EVGNSPDPRA
A-Y49W/E50N/N53R	RVDSAATSGW NIGRPPDYRG	**B-W49Y/N50E/R53N**	VIDSGAVSDY EVGNSPDPRA

2.2.2. Expression and Purification of HCTPT-A and -B Wild Type, Single, Double, and Triple Mutants

E.coli BL21 competent cells were transformed with pET11d::HCPTP-A or pET11d::HCPTP-A single mutants (Y49W or E50N or N53R) or pET11d::HCPTP-A double mutants (Y49W/E50N, E50N/N53R, Y49W/N53R) or pET11d::HCPTP-A triple mutants (Y49W/E50N/N53R). Also, pET11d::HCPTP-B or pET11d::HCPTP-B single mutants (W49Y or N50E or R53N) or pET11d::HCPTP-B double mutants (W49Y/N50E or N50E/R53N or W49Y/R53N) or pET11d::HCPTP-B triple mutants (W49Y/N50E/R53N) were transformed into *E.coli* BL21 competent cells. Single colonies from each transformation were inoculated in 10 mL LB cultures containing 50 ug/ml ampicilin and allowed to grow overnight at 37°C. Overnight 10 mL cultures were used to inoculate flasks containing 1 L LB media, 50 ug/ml ampicilin. LB media is made by dissolving 10 g NaCl, 10 g tryptone, and 5 g yeast extract in 1000 mL deionized water, which is then autoclaved. Cultures were grown at 37°C until an O.D.600 = 0.6 - 0.8 reach. At this point, protein expression was induced by addition of 0.4 mM Isopropyl β-d-1-thiogalactopyranoside (IPTG) in 1 L LB cultures. Cultures were incubated for an additional 16 - 18 hours at 16°C and then, cells were pelleted at 5000 g, 4°C, and then frozen at -20°C.

Frozen cell pellets were resuspended with buffer A that contains 10 mM sodium acetate, 10 mM NaH_2PO_4 and 50 mM NaCl, and 1 mM EDTA at pH 4.8 after which 30ul Dithiothreitol (DTT) and 30ul Phenylmethanesulfonylfluoride (PMSF) were added. The resuspended cells were lysed by three or four passage through a French Press at 1500 psi, after which 100 ul of 100x Halt Protease Inhibitor Cocktali from Thermo Scientific was added. Cell lysates were pelleted at 20,000 rpm for 25 minutes at 4°C.

The supernatants of cell lysate were loaded onto a 20 mL HiPrep 16/10 SP cation exchange column which was pre-equilibrated with buffer A and attached to an AKTA Prime liquid chromatography system. The protein was eluted with a buffer B consisting of 300 mM NaH_2PO_4, 1 mM EDTA at pH 5.1 and baseline was set up according to the protein absorbance at 280 nm. Aliquots from 10 mL fractions collected through the cation exchange chromatography system were analyzed by SDS-PAGE using 15% gels. Fractions including only purified protein were combined and concentrated to about 1.5 - 2 mL using a 10 kDa cutoff spin concentrator at 4500 g and

4°C. Concentrated protein was loaded over a HiPrep 26/60 Sephacryl S-200 size exclusion column which was pre-equilibrated with a buffer A' consisting of 100mM sodium acetate, 10 M EDTA at pH 4.8. Aliquots from10 mL fractions were analyzed by SDS-PAGE 15% gels. Fractions containing only HCPTP were combined and then concentrated to approximately 1.5 - 2 mL through a 10kDa cutoff spin concentrator at 4500 g and 4°C. Concentrated protein containing HCPTP-A and -B, single mutant, double mutant, and triple mutant was stored at 4°C.

2.3. Data and Results

2.3.1. Purification of HCPTP-A and -B, Single, Double, and Triple mutant

The HCPTP-A and -B, single mutant (A-Y49W, E50N, N53R and B-W49Y, N50E, R53N), double mutant (A-Y49W/E50N, E50N/N53R, Y49W/N53R and B-W49Y/N50E, N50E/R53N, W49Y/R53N), and triple mutant (A-Y49W/E50N/N53R and B-W49Y/N50E/R53N) were cloned into pET11d expression vectors and transformed into *E.coli* BL21 competent cells. The induced cultures were lysed by passage through a French Press at 1500 psi and pelleted. Large-scale expression of wild-type and mutant forms of HCPTP-A and -B was followed by a two-step purification involving ion-exchange and size-exclusion chromatography.

The supernatants of cell lysate were purified initially by a HiPrep 16/10 SP cation exchange column as seen in Figure 2.2. - 2.5. Eluted HCPTP-A and -B, single mutant, double mutant, and triple mutant was concentrated and purified again via HiPrep 26/60 Sephacryl S-200 size exclusion choromatography system as seen in Figure 2.6. - 2.9.

The purified protein was concentrated to between 1.5 - 2 mL, which resulted in a HCPTP-A WT concentration of 2.06 mg/ml, A-Y49W concentration of 1.29 mg/ml, A-E50N concentration of 2.33 mg/ml, A-N53R concentration of 1.67 mg/ml, A-Y49W/E50N concentration of 2.05 mg/ml, A-E50N/N53R concentration of 2.2 mg/ml, A-Y49W/N53R concentration of 1.99 mg/ml, A-Y49W/E50N/N53R concentration of 1.63 mg/ml, and in a HCPTP-B WT concentration of 1.73 mg/ml, B-W49Y concentration of 1.71 mg/ml, B-N50E concentration of 1.99 mg/ml, B-R53N concentration of 1.57 mg/ml, B-W49Y/N50E concentration of 1.82 mg/ml, B-N50E/R53N concentration of1.69 mg/ml, B-W49Y/R53N concentration of 2.19 mg/ml, B-W49Y/N50E/R53N concentration of 1.34 mg/ml, respectively. Aliquots of purified HCPTP-A and -B, single, double, and triple mutants were analyzed for purity using SDS-PAGE on a 15% gel as seen in Figure 2.10 - 2.11. Because the molecular weights of HCPTP-A and HCPTP-B are approximately 18 kDa, HCPTP-A and -B, single, double and triple mutants migrated at molecular weight between 15 kDa and 20 kDa, respectively. These purified samples of HCPTP-A and -B,

single, double, triple mutants were used for *p*-Nitrophenyl Phosphate (*p*NPP) assay for measuring each protein activity.

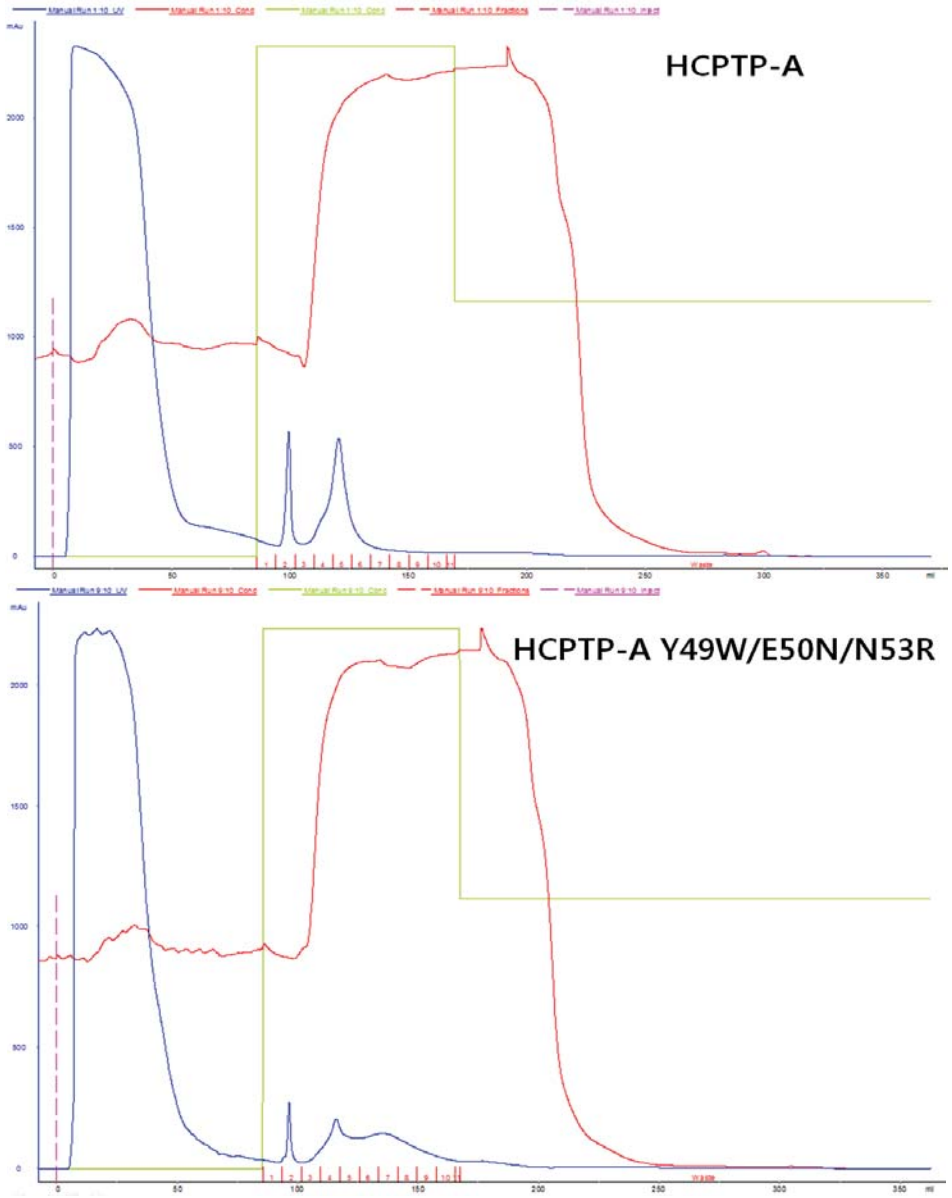

Figure 2.2. Primary purification of HCPTP-A and HCPTP-A Y49W/E50N/N53R using cation exchange chromatography. The supernatants of cell lysate were loaded onto a HiPrep 16/10 SP cation exchange column. Once a baseline was established at 280 nm, protein was eluted off the column and collected in 10 mL fractions. Green lines indicate the shift from 10 mM sodium acetate, 10 mM NaH_2PO_4 and 50 mM NaCl, and 1 mM EDTA at pH 4.8 to 300 mM NaH_2PO_4, 1 mM EDTA at pH 5.1. Blue lines indicate the absorbance at 280 nm.

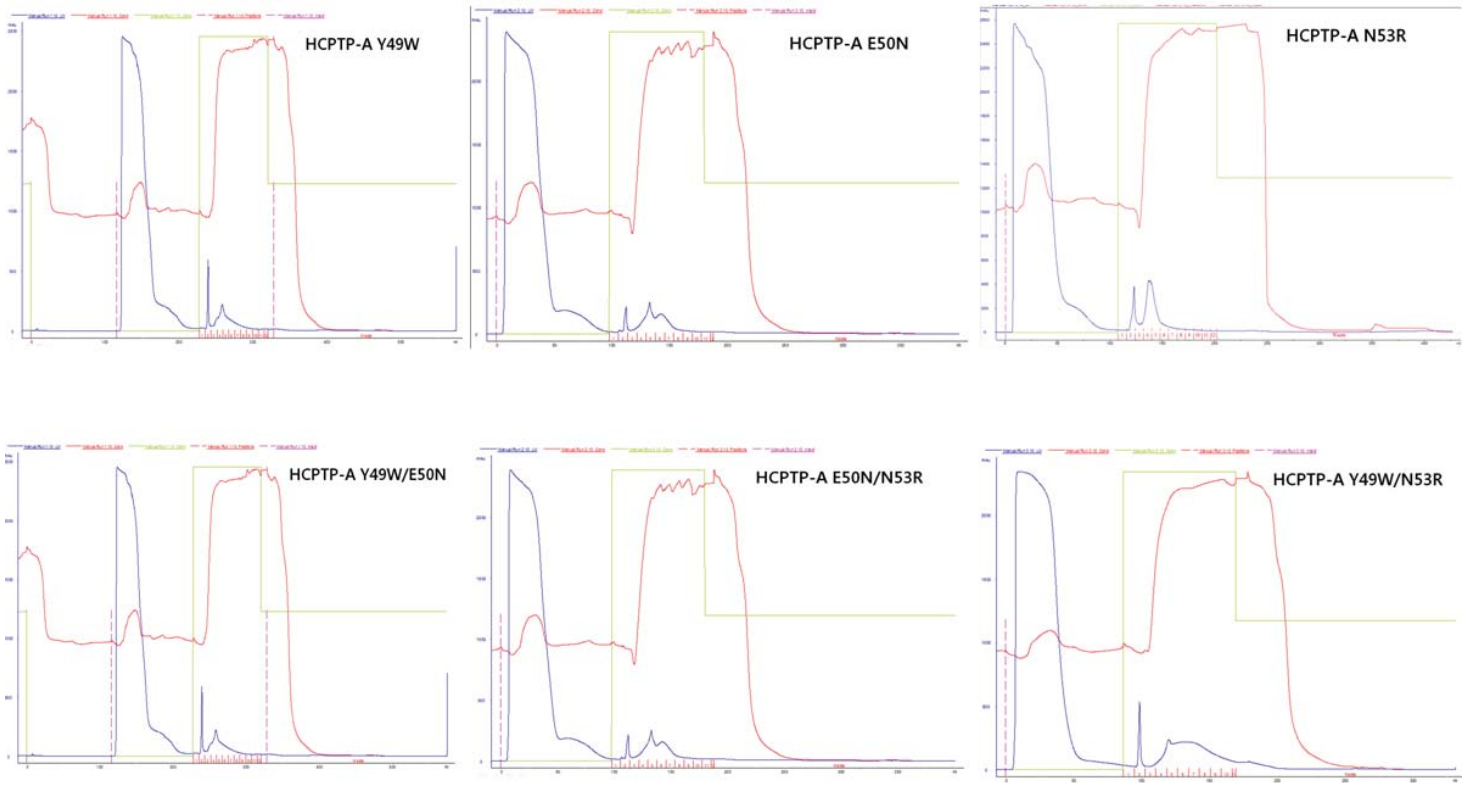

Figure 2.3. Primary purification of HCPTP A-Y49W, E50N, N53R, Y49W/E50N, E50N/N53R, Y49W/N53R using cation exchange chromatography. The supernatants of cell lysate were loaded onto a HiPrep 16/10 SP cation exchange column. Once a baseline was established at 280 nm, protein was eluted off the column and collected in 10 mL fractions. Green lines indicate the shift from 10 mM sodium acetate, 10 mM NaH_2PO_4 and 50 mM NaCl, and 1 mM EDTA at pH 4.8 to 300 mM NaH_2PO_4, 1 mM EDTA at pH 5.1. Blue lines indicate the absorbance at 280 nm.

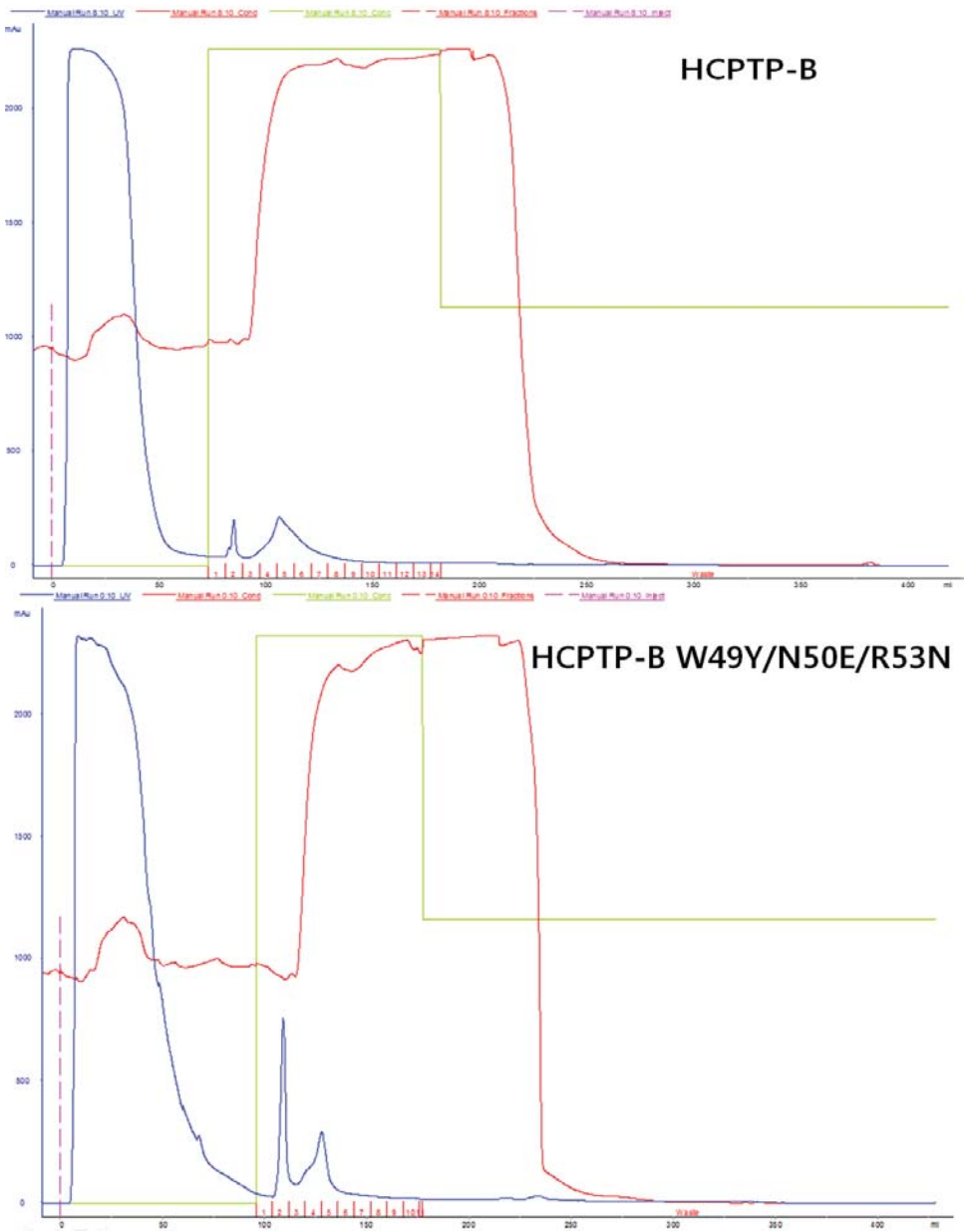

Figure 2.4. Primary purification of HCPTP-B and HCPTP-B W49Y/N50E/R53N using cation exchange chromatography. The supernatants of cell lysate were loaded onto a HiPrep 16/10 SP cation exchange column. Once a baseline was established at 280 nm, protein was eluted off the column and collected in 10 mL fractions. Green lines indicate the shift from 10 mM sodium acetate, 10 mM NaH_2PO_4 and 50 mM NaCl, and 1 mM EDTA at pH 4.8 to 300 mM NaH_2PO_4, 1 mM EDTA at pH 5.1. Blue lines indicate the absorbance at 280 nm.

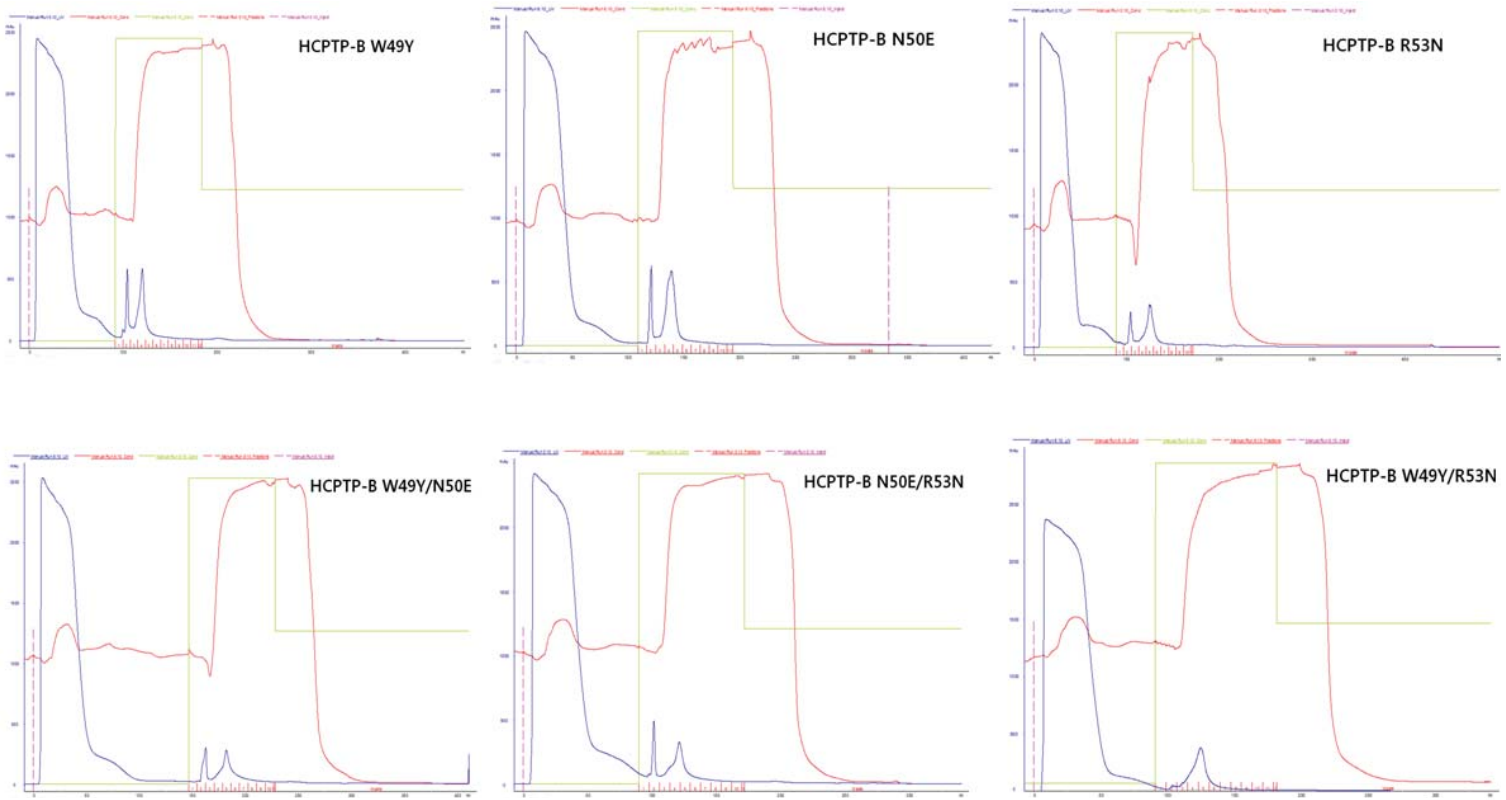

Figure 2.5. Primary purification of HCPTP-B W49Y, N50E, R53N, W49Y/N50E, N50E/R53N, W49Y/R53N using cation exchange chromatography. The supernatants of cell lysate were loaded onto a HiPrep 16/10 SP cation exchange column. Once a baseline was established at 280 nm, protein was eluted off the column and collected in 10 mL fractions. Green lines indicate the shift from 10 mM sodium acetate, 10 mM NaH_2PO_4 and 50 mM NaCl, and 1 mM EDTA at pH 4.8 to 300 mM NaH_2PO_4, 1 mM EDTA at pH 5.1. Blue lines indicate the absorbance at 280 nm.

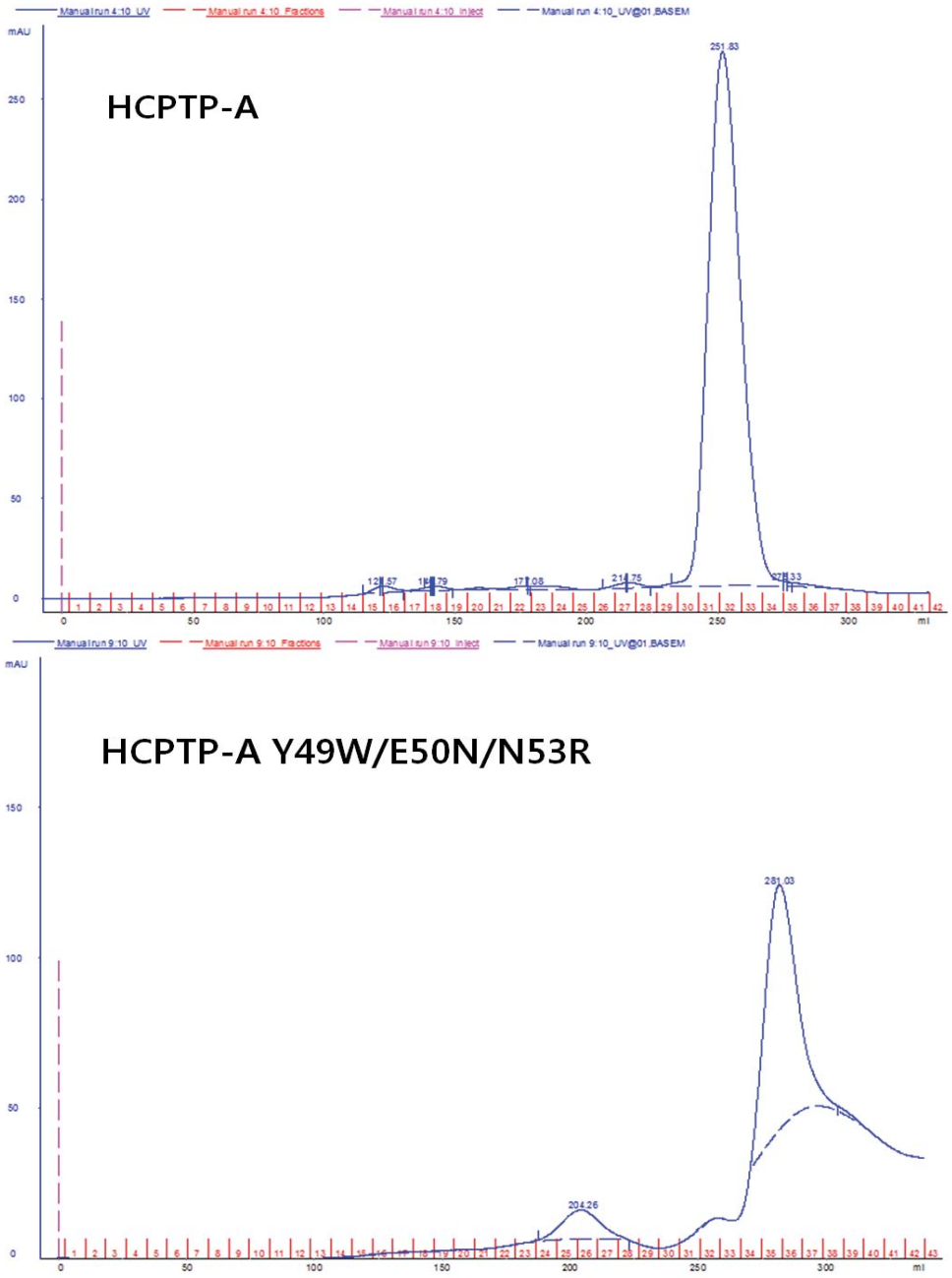

Figure 2.6. Secondary purification of HCPTP-A and HCPTP-A Y49W/E50N/N53R via size exclusion chromatography. The supernatants of cell lysate were loaded onto a HiPrep 26/10 SP Sephacryl S-200 size exclusion column. The protein was eluted off the column and collected in 10 mL fractions. Blue lines indicate the absorbance at 280 nm.

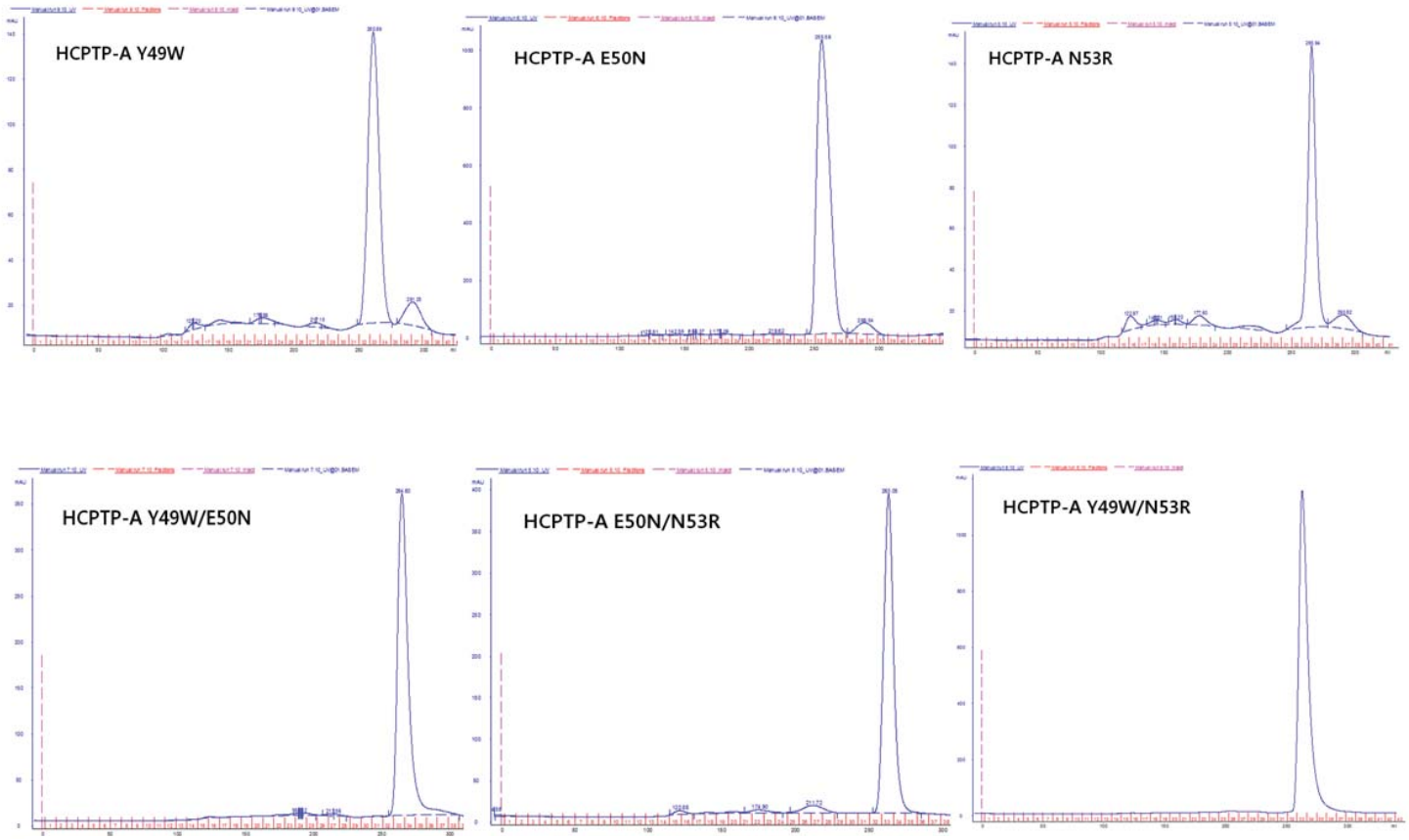

Figure 2.7. Secondary purification of HCPTP-A Y49W, E50N, N53R, Y49W/E50N, E50N/N53R, Y49W/N53R via size exclusion chromatography. The supernatants of cell lysate were loaded onto a HiPrep 26/10 SP Sephacryl S-200 size exclusion column. The protein was eluted off the column and collected in 10 mL fractions. Blue lines indicate the absorbance at 280 nm.

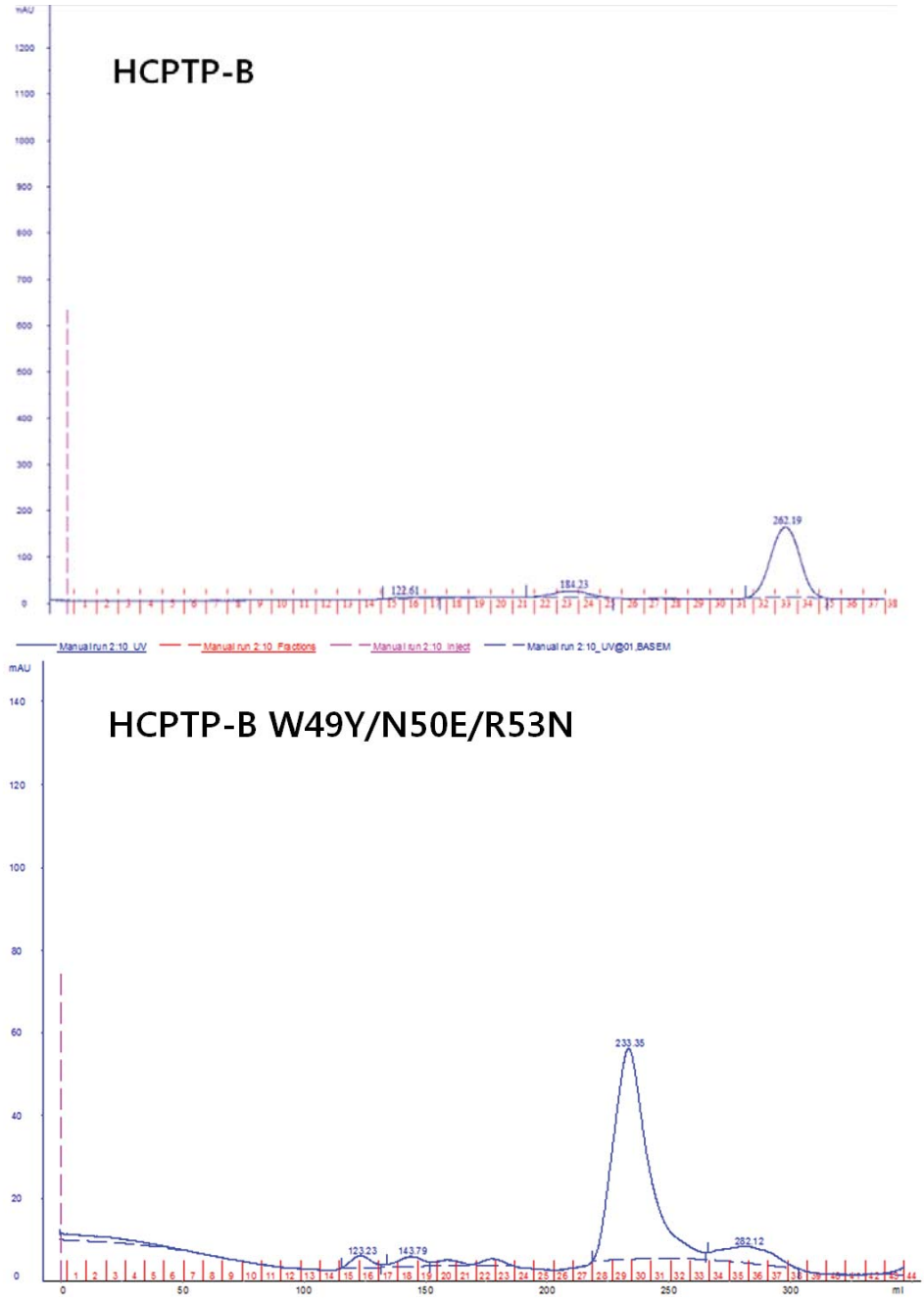

Figure 2.8. Secondary purification of HCPTP-B and HCPTP-B W49Y/N50E/R53N via size exclusion chromatography. The supernatants of cell lysate were loaded onto a HiPrep 26/10 SP Sephacryl S-200 size exclusion column. The protein was eluted off the column and collected in 10 mL fractions. Blue lines indicate the absorbance at 280 nm.

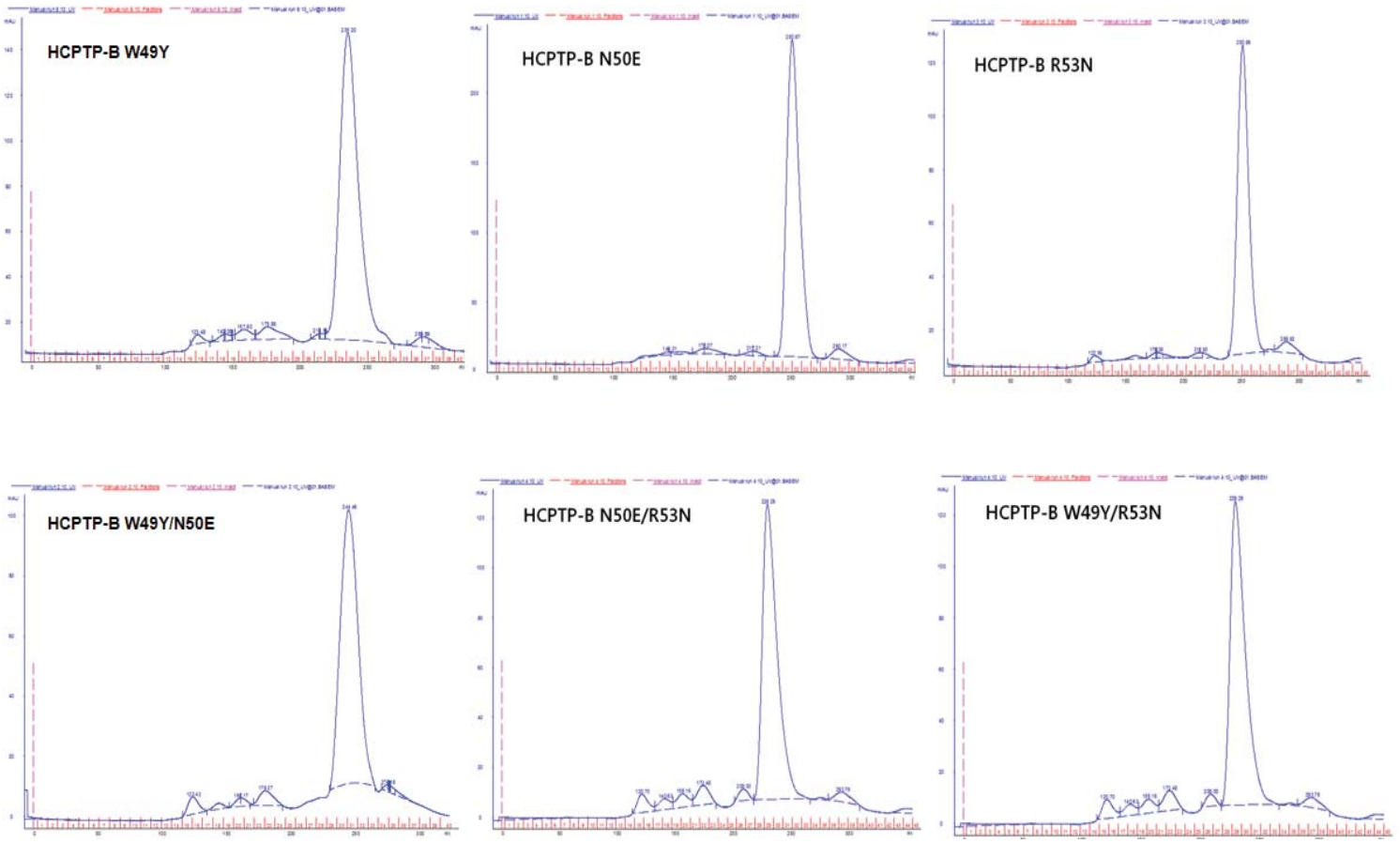

Figure 2.9. Secondary purification of HCPTP-B W49Y, N50E, R53N, W49Y/N50E, N50E/R53N, W49Y/R53N via size exclusion chromatography. The supernatants of cell lysate were loaded onto a HiPrep 26/10 SP Sephacryl S-200 size exclusion column. The protein was eluted off the column and collected in 10 mL fractions. Blue lines indicate the absorbance at 280 nm

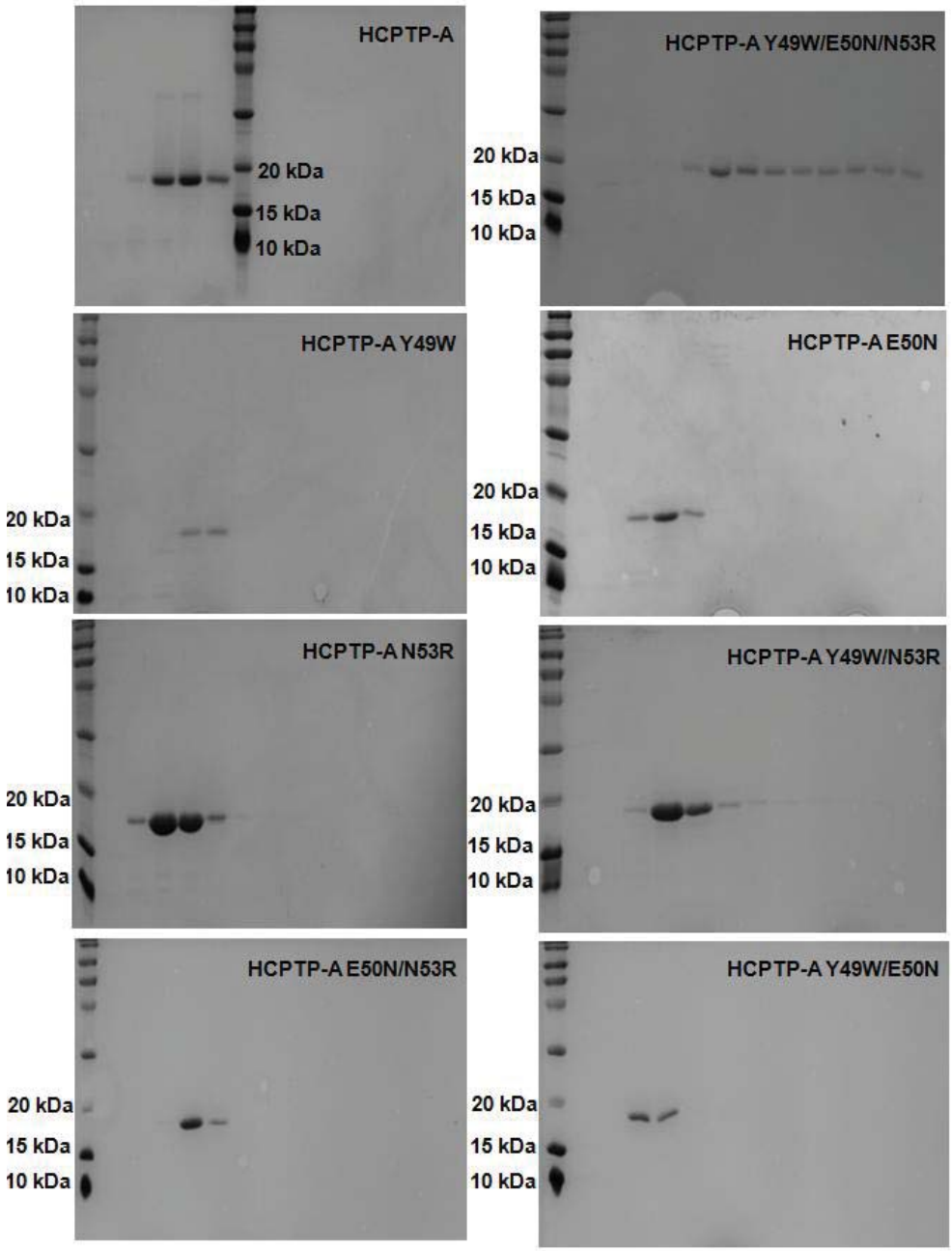

Figure 2.10. SDS-PAGE gel of purified HCPTP-A, A-Y49W, E50N, N53R, Y49W/E50N, E50N/N53R, Y49W/N53R, Y49W/E50N/N53R. 6 ug of each sample were loaded. Lane 1 contains molecular weight markers.

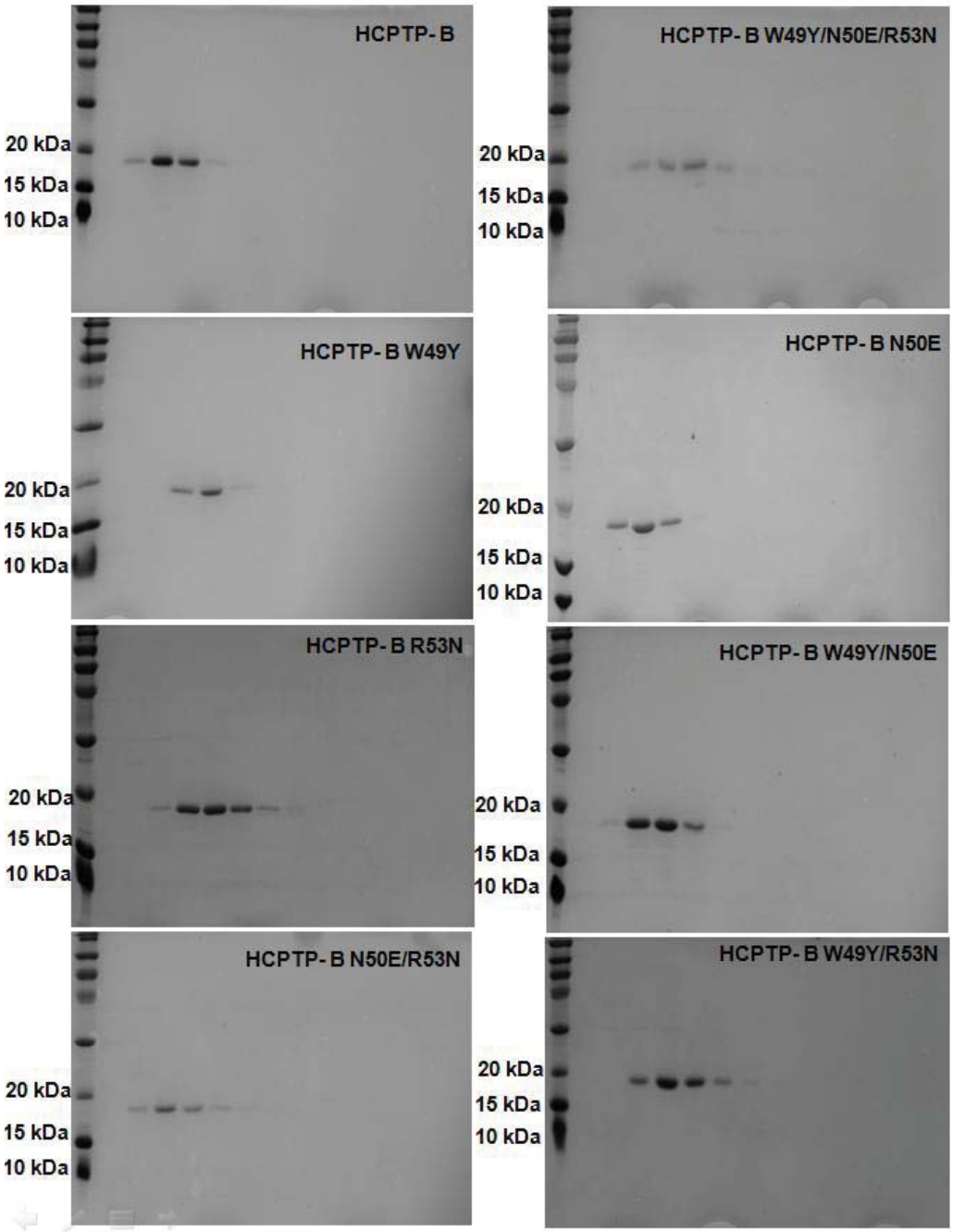

Figure 2.11. SDS-PAGE gel of purified HCPTP-B, B-W49Y, N50E, R53N, W49Y/N50E, N50E/R53N, W49Y/R53N, W49Y/N50E/R53N. 6 ug of each sample were loaded. Lane 1 contains molecular weight markers.

CHAPTER 3. ACTIVITY TEST OF HCPTP-A AND -B, SINGLE, DOUBLE, AND TRIPLE MUTANTS IN PNPP ASSAY

3.1. Introduction

Site-directed mutagenesis was used to examine the role of residues 49, 50, and 53 involved in forming the variable loop of HCPTP-A and -B. Both Glu(E)-50 and Asn(N)-53 in HCPTP-A were mutated to Asn(N)-50 and Arg(R)-53. Tyr(Y)-49 and Asn(N)-53 of HCPTP-A were replaced by Trp(W)-49 and Arg(R)-53. For triple mutant (A-Y49W/E50N/N53R), all three residues, Tyr(Y)-49, Glu(E)-50, and Asn(N)-53, were mutated to Trp(W)-49, Asn(N)-50, and Arg(R)-53 via site-directed mutagenesis. In HCPTP-B N50E /R53N, Asn(N)-50 and Arg(R)-53 were replaced by Glu(E)-50 and Asn(N)-53. Both Trp(W)-49 and Arg(R)-53 in HCPTP-B were mutated to Tyr(Y)-49 and Asn(N)-53. In triple mutant (B- W49Y/N50E/R53N), Trp(W)-49, Asn(N)-50 and Arg(R)-53 were replaced by Tyr(Y)-49, Glu(E)-50 and Asn(N)-53.

Protein tyrosine phosphatases are defined by their ability to hydrolyze the phosphate group from phosphotyrosine. The enzymatic activity of HCPTP-A, Y49W, E50N, N53R, Y49W/E50N, E50N/N53R, Y49W/N53R, Y49W/E50N/N53R, and HCPTP-B, W49Y, N50E, R53N, W49Y/N50E, N50E/R53N, W49Y/R53N, W49Y/N50E/R53N is examined by measuring dephosphorylation of the chromogenic substrate *p*-Nitrophenyl Phosphate at 405 nm.

3.2. Methods

3.2.1. *p*-Nitrophenyl Phosphate Assay (*p*NPP) Test

The enzymatic assays of all HCPTP-A and -B, single, double, and triple mutants were performed at room temperature (21 - 25°C) in 100 mM sodium acetate, 10 mM EDTA, pH 5.0. Each enzyme sample with *p*-Nitrophenyl Phosphate (*p*NPP) in a 1 cm quartz cuvette was monitored using an Ultrospec 3100 pro spectrometer. The reaction was initiated by adding 10 ul of 0.5 uM enzyme with 10 ul *p*NPP (0.1 to 5 K_m) in a 180 ul reaction buffer. The initial velocities were measured by determining the release of *p*-nitrophenolate in a colorimetric procedure with a wavelength of 405 nm and taking the range 0.05 - 1 of absorbance.

For V_{max} and K_m measurements, eight different *p*NPP substrate concentrations (0.1 to 5 K_m) were used and enzyme activity was calculated from the Beer-Lambert Law. The triplicate measurements were made with an extinction coefficient of 1.78×10^4 $M^{-1} \bullet cm^{-1}$ for the standard Michaelis-Menten equation. The values were fitted to the Michaelis-Menten equation and the average and standard derivations of the triplicate assays were calculated.

3.3. Data and Results

V_{max}, K_m (Michaelis constant), K_{cat} (catalytic rate constant), and K_{cat}/K_m values for *p*NPP were determined at pH 5.0 and at room temperature for the HCPTP-A WT, single (Y49W, E50N, N53R), double (Y49W/E50N, E50N/N53R, Y49W/N53R), triple mutant (Y49W/E50N/N53R), and HCPTP-B WT, single (W49Y, N50E, R53N), double (W49Y/N50E, N50E/R53N, W49Y/R53N), triple mutant (W49Y/N50E/R53N). The kinetic data are summarized in Table 4 and Figure 2.12 - 13.

With the substrates *p*NPP, K_m values for HCPTP-A, Y49W, E50N, N53R, Y49W/E50N, E50N/N53R, Y49W/N53R, Y49W/E50N/N53R were 0.22, 0.10, 0.78, 0.10, 0.15, 0.20, 1.44, 0.17 mM, and for HCPTP-B, W49Y, N50E, R53N, W49Y/N50E, N50E/R53N, W49Y/R53N, W49Y/N50E/R53N were 0.66, 0.27, 0.44, 0.34, 0.33, 0.26, 1.01, 0.21 mM, respectively.

Except for A-E50N and A-Y49W/N53R, all of HCPTP-A single, double, and triple mutants showed K_m values that were similar to or less than HCPTP-A wild type. The most striking results were seen for A-E50N, A-Y49W/N53R. The A-E50N and A-Y49W/N53R exhibited 3.5- and 6.5-fold increased K_m values, 0.78 mM and 1.44 mM, compared to the K_m for HCPTP-A of 0.22 mM. Moreover, the K_m for A-E50N (0.78 mM) was more similar to the K_m value for HCPTP-B (0.66 mM) than to HCPTP-A (0.22 mM). Interestingly, except for B-W49Y/R53N which showed an increased K_m value, all HCPTP-B single, double, and triple mutants showed decreased K_m values compared to the HCPTP-B and these decreased K_m for HCPTP-B mutants were similar to the K_m for HCPTP-A. The K_m values for the mutants indicate that the binding interaction of B-W49Y, N50E, R53N, W49Y/N50E, N50E/R53N, W49Y/N50E/R53N may be more similar to the binding interaction of HCPTP-A than to that of the HCPTP-B.

The ratio K_{cat}/K_m shows the catalytic efficiency of enzymes including wild type, single, double, and triple mutant for *p*NPP substrate. The K_{cat}/K_m values for HCPTP-A and HCPTP-B were 0.78 and 0.27 s^{-1} mM^{-1}, respectively.

Interestingly, all HCPTP-A mutants, A-Y49W, E50N, N53R, Y49W/E50N, E50N/N53R, Y49W/N53R, Y49W/E50N/N53R, showed decreased K_{cat}/K_m compared to the HCPTP-A wild type. Moreover, the K_{cat}/K_m value for HCPTP-A Y49W/E50N/N53R is highly decreased compared to the K_{cat}/K_m values for single and double mutants. The K_{cat}/K_m for HCPTP-A Y49W/E50N/N53R (0.48 s^{-1} mM^{-1}) shows that catalytic efficiency of

HCPTP-A Y49W/E50N/N53R is more like HCPTP-B (0.27 s^{-1} mM^{-1}) than HCPTP-A (0.78 s^{-1} mM^{-1}).

Thus, the decreased K_{cat}/K_m values for HCPTP-A Y49W, E50N, N53R, Y49W/E50N, E50N/N53R, Y49W/N53R, especially Y49W/E50N/N53R, compared to HCPTP-A indicate these three mutated residues, Trp(W), Asn(N), and Arg(R) which originated from HCPTP-B, reduce the enzyme efficiency of HCPTP-A.

On the other hand, all HCPTP-B mutants, B-W49Y, N50E, R53N, W49Y/N50E, N50E/R53N, W49Y/R53N, W49Y/N50E/R53N exhibited increased K_{cat}/K_m values compared to the HCPTP-B wild type. The most striking results were seen for B-W49Y and B-N50E. The B-W49Y and B-N50E showed 3- and 2.5-fold increased K_{cat}/K_m values (0.86 and 0.71 $^{-1}$ mM^{-1}) compared to the K_{cat}/K_m for HCPTP-B (0.27 $^{-1}$ mM^{-1}). Moreover, K_{cat}/K_m values for B-W49Y (0.86 $^{-1}$ mM^{-1}) and B-N50E (0.71 $^{-1}$ mM^{-1}) were more similar to K_{cat}/K_m for HCPTP-A (0.78 $^{-1}$ mM^{-1}) than to HCPTP-B (0.27 $^{-1}$ mM^{-1}).

Thus, the increased K_{cat}/K_m values for HCPTP-B R53N, W49Y/N50E, N50E/R53N, W49Y/R53N, W49Y/N50E/R53N, especially W49Y and N50E, over HCPTP-B suggest these three mutated residues, Tyr(Y), Glu(E), and Asn(N), improve catalytic efficiency for HCPTP-B.

Table 4. Kinetic parameters of HCPTP-A and -B, single, double, and triple mutants versus *p*NPP

Data are means ± SE (n=3 independent experiments).

Enzyme	V_{max} (μmol $s^{-1}mg^{-1}$)	K_m (mM)	k_{cat} (s^{-1})	k_{cat}/K_m (s^{-1} mM^{-1})
HCPTP-A	0.99 ± 0.195	0.22 ± 0.035	0.17 ± 0.035	0.78 ± 0.033
HCPTP-B	1.03 ± 0.024	0.66 ± 0.036	0.18 ± 0.004	0.27 ± 0.020
HCPTP-A Y49W	0.28 ± 0.007	0.10 ± 0.009	0.05 ± 0.001	0.50 ± 0.032
HCPTP-A E50N	2.66 ± 0.038	0.78 ± 0.095	0.47 ± 0.007	0.62 ± 0.070
HCPTP-A N53R	0.35 ± 0.002	0.10 ± 0.014	0.06 ± 0.001	0.64 ± 0.106
HCPTP-A Y49W/E50N	0.57 ± 0.012	0.15 ± 0.020	0.10 ± 0.002	0.68 ± 0.069
HCPTP-A E50N/N53R	0.65 ± 0.020	0.20 ± 0.021	0.11 ± 0.004	0.59 ± 0.049
HCPTP-A Y49W/N53R	5.17 ± 0.164	1.44 ± 0.103	0.93 ± 0.029	0.65 ± 0.030
HCPTP-A Y49W/E50N/N53R	0.46 ± 0.018	0.17 ± 0.013	0.08 ± 0.003	0.48 ± 0.039
HCPTP-B W49Y	0.98 ± 0.030	0.27 ± 0.017	0.23 ± 0.061	0.86 ± 0.205
HCPTP-B N50E	1.73 ± 0.040	0.44 ± 0.047	0.31 ± 0.007	0.71 ± 0.063
HCPTP-B R53N	0.73 ± 0.047	0.34 ± 0.007	0.13 ± 0.008	0.37 ± 0.017
HCPTP-B W49Y/N50E	0.88 ± 0.030	0.33 ± 0.042	0.16 ± 0.005	0.48 ± 0.041
HCPTP-B N50E/R53N	0.83 ± 0.029	0.26 ± 0.018	0.15 ± 0.005	0.56 ± 0.027
HCPTP-B W49Y/R53N	2.00 ± 0.090	1.01 ± 0.096	0.36 ± 0.016	0.36 ± 0.017
HCPTP-B W49Y/N50E/R53N	0.63 ± 0.013	0.21 ± 0.022	0.11 ± 0.002	0.53 ± 0.047

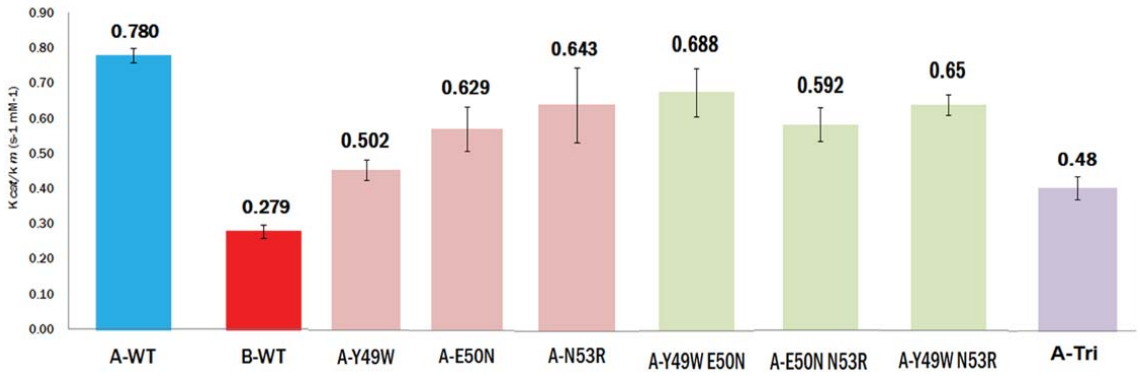

Figure 2.12. K_{cat}/K_m values for HCPTP-A and -B, A-Y49W, E50N, N53R, A-Y49W/E50N, E50N/N53R, Y49W/N53R, A-Y49W/E50N/N53R, respectively.

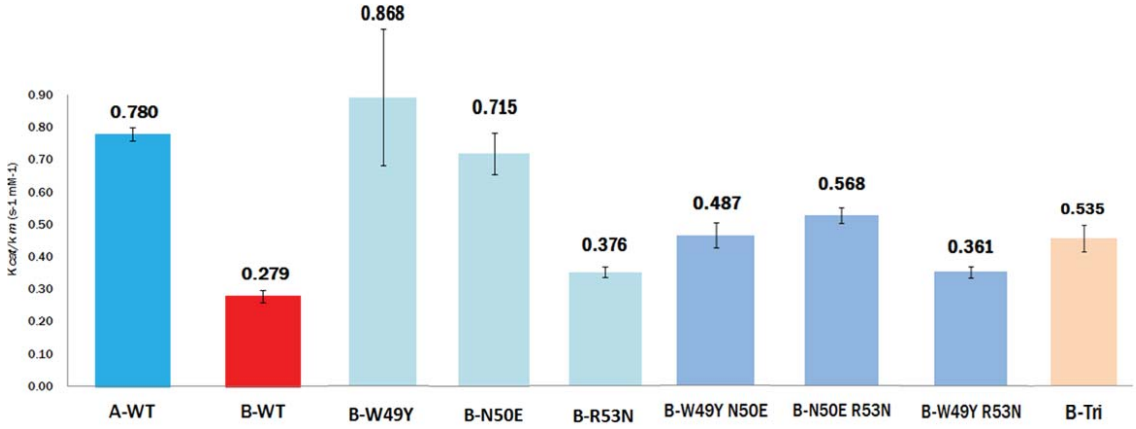

Figure 2.13. K_{cat}/K_m values for HCPTP-A and -B, B-W49Y, N50E, R53N, B-W49Y/N50E, N50E/R53N, W49Y/R53N, and B-W49Y/N50E/R53N, respectively.

3.4. Discussion

Interest in Protein Tyrosine Phosphatases (PTPs) began to rise because PTPs play important roles in the regulation of many cellular signaling pathways including cellular growth, differentiation and metabolism and PTPs emerged as potential drug targets for several disease areas including obesity, cancer, autoimmune and infectious diseases (14) in Table 1.

EphA2 is a receptor tyrosine kinase which is hypo-phosphorylated and overexpressed in many metastatic cancers. The level of phosphorylation of EphA2 is controlled by the human cytoplasmic protein tyrosine phosphatase (HCPTP), which is also overexpressed in cancers (10). This result indicates that HCPTP has oncogenic potential and seems to be responsible for metastatic transformation. Designing specific PTPs inhibitors will ultimately function as potential therapeutic drugs to treat various diseases which are related to deregulation of PTPs.

HCPTP-A and -B are soluble proteins which consist of single polypeptide chains of 157 amino acids and have the PTPase consensus sequence (CX_5R) which forms the active site P loop. The only different sequence between HCPTP-A and -B is an mRNA splice variant sequence including amino acids 40 - 73 which forms the variable loop (8). HCPTP-A and HCPTP-B show different activity towards inhibitors and phosphotyrosine peptides (7). HCPTP-A has a higher activity towards phosphotyrosine, *p*-nitrophenyl phosphate (*p*NPP) and inhibitors, while HCPTP-B shows a lower response to *p*NPP and phosphotyrosine as well as inhibitors. Moreover, HCPTP-A and HCPTP-B dephosphorylate different phosphotyrosine sites related to control of EphA2 activity and downstream signaling pathways (9).

Based on the preliminary study, our lab identified three potential variable loop residues (49, 50, and 53) which may influence substrate binding and catalytic efficiency of HCPTP-A and -B (7). The first one is Tyr(Y)-49 in HCPTP-A and Trp(W)-49 in HCPTP-B, located above the active site forming the hydrophobic sandwich with Tyr(Y)-131 and -132, which affects interaction of the phosphotyrosine substrates. The second is Glu(E)-50 in HCPTP-A, which contains a negatively charged side chain, whereas, Arg(R)-53 in HCPTP-B, possesses a positively charged side chain. These two residues, 50 and 53, play critical roles in the interaction of enzymes and substrates recognized by their charge distribution.

With the substrate *p*NPP, HCPTP-A (0.22 mM) showed 3-fold decreased K_m value compared to the K_m for HCPTP-B (0.66 mM). Because the K_m is dissociation constant, this result suggests that HCPTP-A binds three times more tightly to *p*NPP than HCPTP-B. On the other hand, K_{cat}/K_m value, the catalytic efficiency towards *p*NPP substrate, for HCPTP-A (0.78 s^{-1} mM^{-1}) increased approximately 3-times compared to the K_{cat}/K_m for HCPTP-B (0.27 s^{-1} mM^{-1}) even though K_{cat} value for HCPTP-A and -B were similar to each other (0.17 s^{-1} and 0.18 s^{-1}). Thus, these data indicate that HCPTP-A has more efficient enzymatic and catalytic activity towards *p*NPP than HCPTP-B.

Except for A-E50N and A-Y49W/N53R, all HCPTP-A single, double, and triple mutants showed K_m values which were similar to or less than HCPTP-A WT. These results were unexpected. Interestingly, K_{cat} values for all HCPTP-A single, double, and triple mutants is highly decreased compared to HCPTP-A WT, but A-E50N and A-Y49W/N53R. Thus, three residues, Trp(W), Asn(N), and Arg(R) which originated from HCPTP-B, are more likely affect on enzyme turn-over number (K_{cat}) than enzyme affinity toward substrate.

On the other hand, except for B-W49Y/R53N, all HCPTP-B single, double, and triple mutants showed 2- and 3-times decreased K_m values in comparison to HCPTP-B. These decreased K_m for HCPTP-B single, double, and triple mutants were similar to the K_m value for HCPTP-A, which suggests that the binding interaction of B-W49Y, N50E, R53N, W49Y/N50E, N50E/R53N, W49Y/N50E/R53N may be more similar to the binding interaction of HCPTP-A than to that of HCPTP-B. Thus, mutated three residues, Tyr(Y), Glu(E), and Asn(N) which derived from HCPTP-A, seems to enhance binding interaction of HCPTP-B for *p*NPP substrate.

Interestingly, all HCPTP-A single (Y49W, E50N, N53R), double (Y49W/E50N, E50N/N53R, Y49W/N53R), and triple mutant (Y49W/E50N/N53R) showed decreased K_{cat}/K_m values in comparison to HCPTP-A WT. The most striking results were seen for A-Y49W/E50N/N53R. The K_{cat}/K_m value for A-Y49W/E50N/N53R is 1.6-fold decreased than HCPTP-A WT. The HCPTP-A Y49W/E50N/N53R shows K_{cat}/K_m value (0.48 s^{-1} mM^{-1}) more like HCPTP-B (0.27 s^{-1} mM^{-1}) than HCPTP-A (0.78 s^{-1} mM^{-1}). The decreased K_{cat}/K_m values for HCPTP-A single mutants (Y49W, E50N, N53R), double mutants (Y49W/E50N, E50N/N53R, Y49W/N53R), and especially triple mutant (Y49W/E50N/N53R) compared to the K_{cat}/K_m for HCPTP-A WT shows that three mutated

residues, Trp(W), Asn(N), and Arg(R) which originated from HCPTP-B WT, seems to affect enzymatic activity and especially reduce catalytic efficiency for HCPTP-A. All HCPTP-B single (W49Y, N50E, R53N), double (W49Y/N50E, N50E/R53N, W49Y/R53N), and triple mutant (W49Y/N50E/R53N) showed increased K_{cat}/K_m values over the HCPTP-B WT. Especially, B-W49Y and B-N50E showed 3- and 2.5-fold increased K_{cat}/K_m values (0.86 and 0.71 s^{-1} mM^{-1}) compared to the K_{cat}/K_m for HCPTP-B (0.27 s^{-1} mM^{-1}). These increased K_{cat}/K_m for B-W49Y (0.86 s^{-1} mM^{-1}) and B-N50E (0.71 s^{-1} mM^{-1}) were more similar to the K_{cat}/K_m value for HCPTP-A (0.78 s^{-1} mM^{-1}) than to HCPTP-B (0.27 s^{-1} mM^{-1}). Moreover, the K_{cat}/K_m for HCPTP-B triple mutant (0.53 s^{-1} mM^{-1}) was also more similar to HCPTP-A (0.78 s^{-1} mM^{-1}) than to HCPTP-B (0.27 s^{-1} mM^{-1}). The increased K_{cat}/K_m for HCPTP-B R53N, double (W49Y/N50E, N50E/R53N, W49Y/R53N), and triple mutant (W49Y/N50E/R53N), especially W49Yand N50E compared to HCPTP-B WT indicates that the three mutated residues, Tyr(Y), Glu(E), and Asn(N) that originated from HCPTP-A, seems to improve catalytic efficiency and enzyme activity of HCPTP-B.

Taken together, these results are consistent with the hypothesis that the three variable loop residues (Tyr(Y)-49, Glu(E)-50, Asn(N)-53 in HCPTP-A and Trp(W)-49, Asn(N)-50, Arg(R)-53 in HCPTP-B) are the key residues affecting the substrate binding for HCPTP-A and HCPTP-B and these three residues play a significant role in enzymatic activity.

For a better investigation of the effect of three potential variable loop residues (positions 49, 50, and 53) of HCPTP-A and HCPTP-B, additional research including Malachite Green Assay with phosphotyrosine peptides (derived from the EphA2) at physiological conditions (pH 7 and 37°C) is needed as *p*NPP substrate is a synthetic molecule of smaller size which can easily enter and leave active site of enzyme. Using biological substrate such as phosphotyrosine peptides originated from the EphA2 will provide a more detailed understanding of the physiological function of HCTPT-A and HCPTP-B. In addition, future research measuring the dissociation constant (K_i), with inhibitors will also provide characteristics of specific residues that control the affinity of substrates for the HCPTP-A and HCPTP-B.

BIBLIOGRAPHY

BIBLIOGRAPHY

1) Dissing J, Dahl O, Svensmark O (1979) Phosphonic and arsonic acids as inhibitors of human red cell acid phosphatase and their use in affi nity chromatography. Biochim Biophys Acta 569:159–176.

2) Bryson GL, Massa H, Trask BJ, Van Etten RL (1995) Gene structure, sequence, and chromosomal localization of the human red cell-type low-molecular-weight acid phosphotyrosyl phosphatase gene, ACP1. Genomics 30:133–140.

3) Stephanie M. Stanford , Massimo Bottini , and Nunzio Bottini Al-Chalabi (2013) The Role of LMPTP in the Metabolic Syndrome. Protein Tyrosine Phosphatase Control of Metabolism DOI 10.1007/978-1-4614-7855-3_11.

4) Rudbeck L, Dissing J, Lazaruk KD, Sensabaugh G (2000) Human 18 kDa phosphotyrosine protein phosphatase (ACP1) polymorphism: studies of rare variants provide evidence that substitutions within or near alternatively spliced exons affect splicing result. Ann Hum Genet 64:107–116

5) Tailor P, Gilman J, Williams S, Mustelin T (1999) A novel isoform of the low molecular weight phosphotyrosine phosphatase, LMPTP-C, arising from alternative mRNA splicing. Eur J Biochem 262:277–282

6) Zhang, Z. Y., and Van Etten, R. L. (1990) Arch. Biochem. Biophys. 282, 39–49

7) Adam P.R. Zabell, Alfred D. Schroff, Jr, Bornadata Evans Bains, Robert L. Van Etten, Olaf Wiest, and Cynthia V. Stauffacher (2005) Crystal structure of the Human B-form Low Molecular Weight Phosphotyrosyl Phosphatase at 1.6-A Resolution. Journal of Biological Chemistry.281, 10.

8) Marie Zhang, Cynthia V. Stauffacher, Dayin Lin, and Robert L. Van Etten. (1998) Crystal structure of a human low molecular weight phosphotyrosyl phosphatase. 273. 21714-21720

9) Balasubramaniam D, Paul LN, Homan KT, Hall M, and Stauffacher CV. Protein Science. 2011. 20: 1172-1181.

10) Kikawa KD, Vidale DR, Van Etten RL, Kinch MS (2002) Regulation of the EphA2 kinase by the low molecular weight tyrosine phosphatase induces transformation.J Biol Chem 277:39274–39279

11) Shultz LD, Schweitzer PA, Rajan TV, Yi T, Ihle JN, Matthews RJ, Thomas ML, Beier DR: Mutations at the murine motheaten locus are within the hematopoietic cell protein tyrosine phosphatase (hcph) gene. Cell 1993, 73:1445-1454.

12) Pingel JT, Thomas ML: Evidence that the leukocyte-common antigen is required for antigen-induced T lymphocyte proliferation. Cell 1989, 58:1055-1065.

13) Elchebly M, Payette P, Michaliszyn E, Cromlish W, Collins S, Loy AL, Normandin D, Cheng A, Himms-Hagen J, Chan CC et al.: Increased insulin sensitivity and obesity resistance in mice lacking the protein tyrosine phosphatase-1B gene. Science 1999, 283:1544-1548.

14) Rob Hooft van Huijsduijnen, Agnes Bombrun and Dominique Swinnen. (2002). Selecting protein tyrosine phophatases as drug targets. Therapeutic focus. review. 7, 1013-1018.